ANALYSIS OF CAPSULE D FROM THE CONNECTICUT YANKEE REACTOR VESSEL RADIATION SURVEILLANCE PROGRAM (WCAP-10236)

EPRI RESEARCH PROJECT 1021-3
TOPICAL REPORT

S. E. Yanichko
S. L. Anderson
R. P. Shogan
R. G. Lott

JANUARY 1983

Prepared by

WESTINGHOUSE ELECTRIC CORPORATION
Nuclear Technology Division
P. O. Box 355
Pittsburgh, Pennsylvania 15230

T. R. Mager, Principal Investigator

Prepared for

ELECTRIC POWER RESEARCH INSTITUTE
3412 Hillview Avenue
Palo Alto, California 94304

T. U. Marston, Project Manager

LEGAL NOTICE

This report was prepared by Westinghouse Electric Corporation (WESTINGHOUSE) as an account of work sponsored by the Electric Power Research Institute, Inc. (EPRI). Neither EPRI, members of EPRI, nor WESTINGHOUSE, nor any person acting on behalf of either:

a. Makes any warranty or representation, express or implied, with respect to the accuracy, completeness, or usefulness of the information contained in this report, or that the use of any information, apparatus, method, or process disclosed in this report may not infringe privately owned rights; or

b. Assumes any liabilities with respect to the use of, or for damages resulting from the use of, any information, apparatus, method, or process disclosed in this report.

TABLE OF CONTENTS

LIST OF TABLES

LIST OF TABLES (cont)

LIST OF ILLUSTRATIONS

LIST OF ILLUSTRATIONS (cont)

SECTION 1
SUMMARY OF RESULTS

The analysis of the reactor vessel material contained in the fourth reactor vessel material surveillance capsule which was removed from the Connecticut Yankee reactor pressure vessel after approximately 10.5 effective full power years of operation led to the following conclusions:

- The capsule received an average fast neutron fluence ($E > 1$ Mev) of $2.22 \times 10^{19} n/cm^2$ compared to a calculated fluence of $2.39 \times 10^{19} n/cm^2$.

- Irradiation of base metal plate material to $2.22 \times 10^{19} n/cm^2$ resulted in a 43° C increase in the 41-Joule transition temperature when compared with unirradiated values. This transition temperature increase, when compared with increases of 44 and 37° C obtained for earlier capsules irradiated to 0.471 and $1.58 \times 10^{19} n/cm^2$ respectively indicates that the base material is experiencing a saturation of radiation damage.

- Reactor vessel submerged arc weld metal irradiated to $2.22 \times 10^{19} n/cm^2$ showed a 41-Joule transition temperature increase of 61° C which was only 8° C higher than the increase obtained on weld metal irradiated at $0.239 \times 10^{19} n/cm^2$. The small transition temperature increase for these two irradiation fluence levels indicate that saturation of radiation damage is occurring for the weld metal.

- Comparisons of the 41-Joule transition temperature increases for the Connecticut Yankee materials with Regulatory Guide 1.99 Revision 1 predictions show that the increases after irradiation to $2.22 \times 10^{19} n/cm^2$ are significantly less than predicted.

- End-of-life projected maximum fast neutron fluences for the reactor vessel based on 27 effective full power years of operation at 1825 MWt are as follows:

	Fast Neutron Fluence (n/cm^2)	
Vessel Location	**Calculated**	**Measured**
Inner Surface	6.3×10^{19}	5.9×10^{19}
1/4 Thickness	2.9×10^{19}	2.7×10^{19}
3/4 Thickness	4.1×10^{19}	3.8×10^{19}

SECTION 2
INTRODUCTION

This report presents the results of the examination of Capsule D, the fourth capsule to be removed from the reactor in the continuing surveillance program which monitors the effects of neutron irradiation on the Connecticut Yankee reactor pressure vessel materials under actual operating conditions.

The surveillance program for the reactor pressure vessel materials was designed and recommended by the Westinghouse Electric Corporation. A description of the surveillance program and the preirradiation mechanical properties of the reactor vessel materials are presented in WCAP-7036[1]. The surveillance program was planned to cover the 30-year life of the reactor pressure vessel and was based on ASTM E185-62. Westinghouse Nuclear Technology Division personnel were contracted for the preparation of procedures for removing the capsule from the reactor and its shipment to the Westinghouse Research and Development Laboratory, where the postirradiation mechanical testing of the Charpy V-notch impact and tensile surveillance specimens was performed.

This report summarizes testing and the postirradiation data obtained from the fourth surveillance capsule (Capsule D) removed from the Connecticut Yankee reactor vessel and discusses the analysis of these data. The data are also compared to results obtained from the three previous surveillance capsules (Capsules A, F and H)[2, 3, 4] which were tested as part of the program.

SECTION 3
BACKGROUND

The ability of the large steel pressure vessel containing the reactor core and its primary coolant to resist fracture constitutes an important factor in ensuring safety in the nuclear industry. The beltline region of the reactor pressure vessel is the most critical region of the vessel because it is subjected to significant fast neutron bombardment. The overall effects of fast neutron irradiation on the mechanical properties of low alloy ferritic pressure vessel steels such as SA302 Grade B (base material of Connecticut Yankee reactor pressure vessel beltline) are well documented in the literature. Generally, low alloy ferritic materials show an increase in hardness and tensile properties and a decrease in ductility and toughness under certain conditions of irradiation.

A method of performing analyses to guard against fast fracture in reactor pressure vessels has been presented in "Protection Against Non-ductile Failure," appendix G to section III of the ASME Boiler and Pressure Vessel Code. The method utilizes fracture mechanics concepts and is based on the reference nil-ductility temperature RT_{NDT}.

RT_{NDT} is defined as the greater of either the drop weight nil-ductility transition temperature (NDTT per ASTM E-208) or the temperature 60° F less than the 50 ft.lb. (and 35 mils lateral expansion) temperature as determined from Charpy specimens oriented normal to the major working direction of the material. The RT_{NDT} of a given material is used to index that material to a reference stress intensity factor curve (K_{IR} curve) which appears in appendix G of the ASME Code. The K_{IR} curve is a lower bound of dynamic, crack arrest, and static fracture toughness results obtained from several heats of pressure vessel steel. When a given material is indexed to the K_{IR} curve, allowable stress intensity factors can be obtained for this material as a function of temperature. Allowable operating limits can then be determined utilizing these allowable stress intensity factors.

RT_{NDT} and, in turn, the operating limits of nuclear power plants can be adjusted to account for the effects of radiation on the reactor vessel material properties. The radiation embrittlement or changes in mechanical properties of a given reactor pressure vessel steel can be monitored by a reactor surveillance program such as the Connecticut Yankee Reactor Vessel Radiation Surveillance Program, [1] in which a surveillance capsule is periodically removed from the operating nuclear reactor and the encapsulated specimens are tested. The increase in the Charpy V-notch 50 ft. lb. temperature (ΔRT_{NDT}) due to irradiation is added to the original RT_{NDT} to adjust the RT_{NDT} for radiation embrittlement. This adjusted RT_{NDT} (RT_{NDT} initial + ΔRT_{NDT}) is used to index the material to the K_{IR} curve and, in turn, to set operating limits for the nuclear power plant which take into account the effects of irradiation on the reactor vessel materials.

SECTION 4
DESCRIPTION OF PROGRAM

Eight surveillance capsules for monitoring the effects of neutron exposure on the Connecticut Yankee reactor pressure vessel core region material were inserted in the reactor vessel prior to initial plant startup. The eight capsules were positioned in the reactor vessel between the thermal shield and the vessel wall at locations shown in Figure 4-1. The vertical center of the capsules is opposite the vertical center of the core.

Capsule D was removed after approximately 10.5 effective full power years of plant operation. This capsule shown in Figure 4-2, contained Charpy V-notch impact, tension and IX-wedge opening loading (WOL) fracture mechanics specimens from the vessel intermediate shell plate W9807-4 and submerged arc weld metal representative of the core region of the reactor vessel and Charpy V-notch specimens from weld heat-affected zone (HAZ) material. The capsule also contained Charpy V-notch specimens from the 6-inch-thick ASTM correlation monitor material (A302 Grade B). The chemistry and heat treatment of the surveillance materials are presented in Table 4-1. The chemical analyses reported in Table 4-1 were obtained from unirradiated material used in the surveillance program. In addition a chemical analysis was performed on an irradiated Charpy specimen from the weld metal and is also reported in Table 4-1. The analysis of the irradiated weld metal indicates that the copper, nickel and phosphorus contents are in good agreement with the unirradiated analysis.

Test specimens from the plate material were machined from the 1/4 thickness location of the plate. Test specimens represent material taken at least one plate thickness from the quenched end of the plate. All base metal Charpy V-notch and tension specimens were oriented with the longitudinal axis of the specimen parallel to the principle rolling direction of the plate. Charpy V-notch and tension specimens from the weld metal were oriented with the longitudinal axis of the specimens transverse to the welding direction.

Capsule D contained dosimeter wires of pure copper, nickel and aluminum-0.15 Wt%-cobalt (cadmium - shielded and unshielded). In addition, cadmium-shielded dosimeters of Np^{237} and U^{238} were contained in the capsule. The test specimens served as iron dosimeters. Thermal monitors made from two low melting eutectic alloys sealed in quartz tubes were included in the capsule and were located as shown in Figure 4-2. The two eutectic alloys and their melting points are:

2.5% Ag, 97.5% Pb	Melting Point 579° F (304° C)
1.75% Ag, 0.75% Sn, 97.5% Pb	Melting Point 590° F (310° C)

TABLE 4-1

CHEMICAL COMPOSITION AND HEAT TREATMENT OF MATERIAL FOR THE CONNECTICUT YANKEE REACTOR VESSEL SURVEILLANCE PROGRAM

Chemical Composition (percent)						
Element	**Plate W9807-2**	**Plate W9807-4**	**Plate W9807-7**	**Weld Metal**		**Correlation Monitor**
C	0.20	0.20	0.20	0.047	—	0.24
Mn	1.42	1.37	1.46	1.36	1.34	1.34
P	0.010	0.010	0.013	0.020	0.015	0.011
S	0.014	0.021	0.010	0.019	—	0.023
Si	0.26	0.19	0.22	0.35	0.29 [a]	0.23
Mo	0.47	0.47	0.48	0.48	0.34	0.51
Cu	0.10	0.12	0.12	0.22	0.19	0.20
Ni	—	—	—	0.046	0.042	0.18
Cr	—	—	—	—	0.061	0.11

a. Analysis performed on Charpy Weld Specimen D-9 from Capsule D

Heat Treatment	
Base Plates	Heated to 1550-1600° F - 4 hr, water quenched Tempered at 1225° F - 4 hr, furnace cooled Stress relieved at 1150° F - 24 hr, furnace cooled
Weld Metal	Stress relieved at 1150° F - 24 hr, furnace cooled
ASTM A302B Correlation Monitor	Heated to 1650° F - 4 hr, water quenched to 300° F Tempered at 1200° F - 6 hr, air cooled

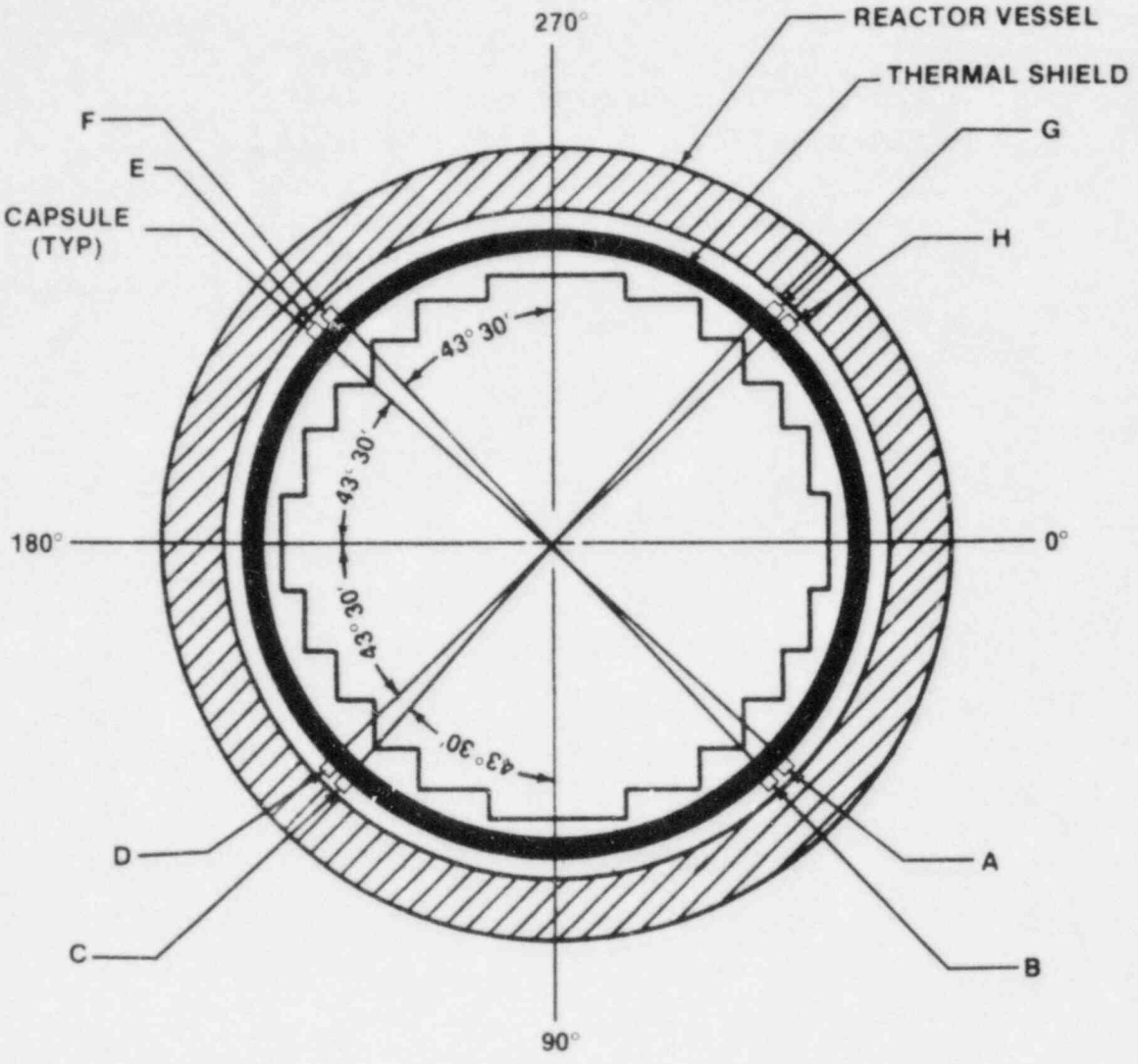

Figure 4-1. Arrangement of Surveillance Capsules in the Connecticut Yankee Reactor Vessel

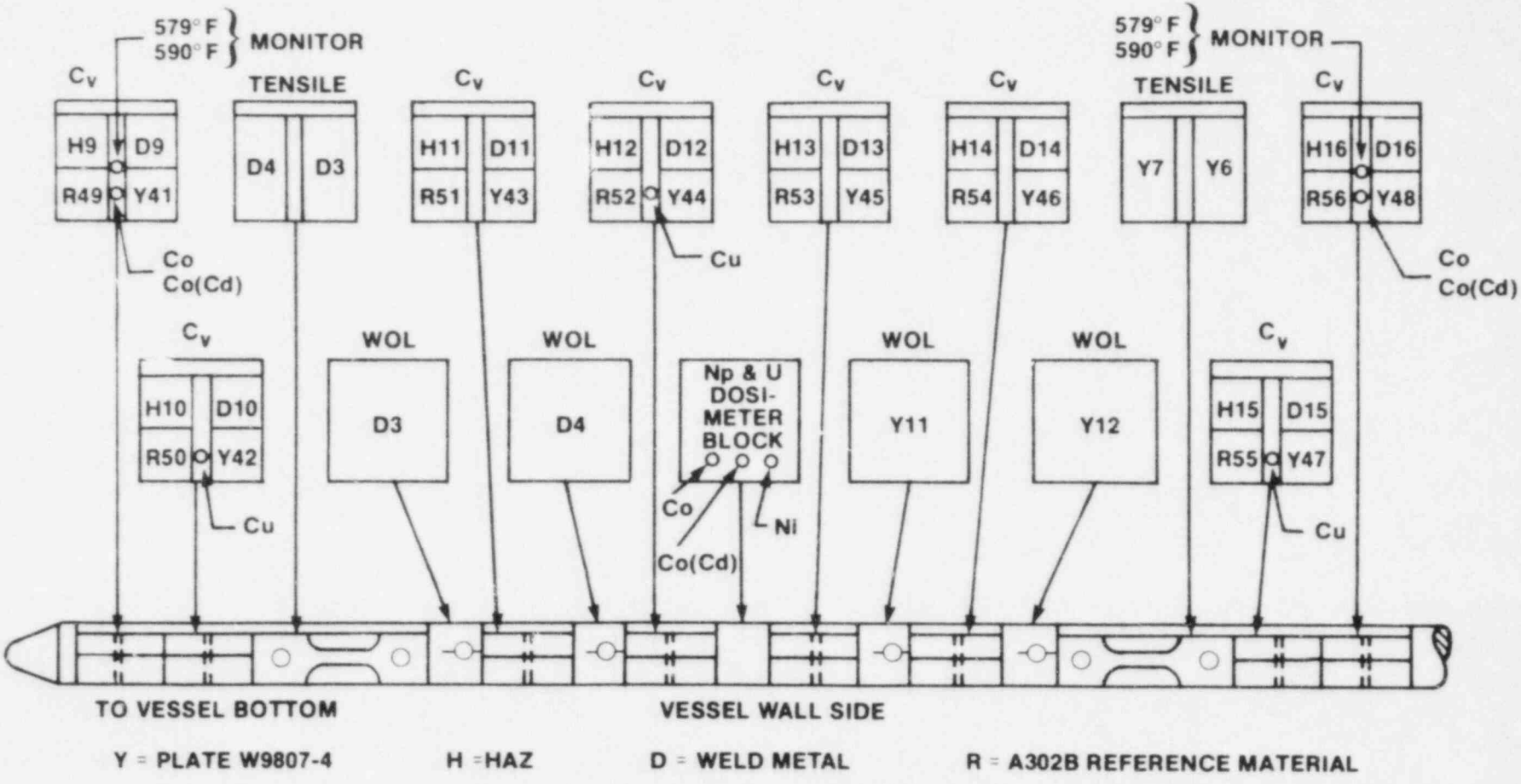

Figure 4-2. Arrangement of Specimens, Thermal Monitors, and Dosimeters in Capsule D

SECTION 5
TESTING OF SPECIMENS FROM CAPSULE D

5-1. OVERVIEW

The postirradiation mechanical testing of the Charpy V-notch and tension specimens was performed at the Westinghouse Research and Development Laboratory consultation by Westinghouse Nuclear Energy Systems personnel. Testing was performed in accordance with 10CFR50, Appendices G and H.

Upon receipt of the capsule at the laboratory, the specimens and spacer blocks were carefully removed, inspected for identification number, and checked against the master list in WCAP-7036.[1] No discrepancies were found.

Examination of the two low-melting 304° C (579° F) and 310° C (590° F) eutectic alloys indicated no melting of either type of thermal monitor. Based on this examination, the maximum temperature to which the test specimens were exposed was less than 304° C (579° F).

The Charpy impact tests were performed on a Tinius-Olsen Model 74,358J machine. The tup (striker) of the Charpy machine is instrumented with an Effects Technology model 500 instrumentation system. With this system, load-time and energy-time signals can be recorded in addition to the standard measurement of Charpy energy (E_D). From the load-time curve, the load of general yielding (P_{GY}), the time to general yielding (t_{GY}), the maximum load (P_M), and the time to maximum load (t_M) can be determined. Under some test conditions, a sharp drop in load indicative of fast fracture was observed. The load at which fast fracture was initiated is identified as the fast fracture load (P_F), and the load at which fast fracture terminated is identified as the arrest load (P_A).

The energy at maximum load (E_M) was determined by comparing the energy-time record and the load-time record. The energy at maximum load is roughly equivalent to the energy required to initiate a crack in the specimen. Therefore, the propagation energy for the crack (E_p) is the difference between the total energy to fracture (E_D) and the energy at maximum load.

The yield stress (σ_y) is calculated from the three point bend formula. The flow stress is calculated from the average of the yield and maximum loads, also using the three point bend formula.

Percent shear was determined from postfracture photographs using the ratio-of-areas method in compliance with ASTM Specification A370-74. The lateral expansion was measured using a dial gage rig similar to that shown in the same specification.

Tension tests were performed on a 20,000-pound Instron, split-console test machine (Model 1115) per ASTM Specifications E8 and E21, and MHL Procedure 7604 Revision 2. All pull rods, grips, and pins were made of Inconel 718 hardened to R_C45. The upper pull rod was connected through a universal joint to improve axiality of loading. The tests were conducted at a constant crosshead speed of 0.05 inch per minute throughout the test.

Deflection measurements were made with a linear variable displacement transducer (LVDT) extensometer. The extensometer knife edges were spring-loaded to the specimen and operated through specimen failure. The extensometer gage length is 1.00 inch. The extensometer is rated as Class B-2 per ASTM E83.

Elevated test temperatures were obtained with a three-zone electric resistance split-tube furnace with a 9-inch hot zone. All tests were conducted in air.

Because of the difficulty in remotely attaching a thermocouple directly to the specimen, the following procedure was used to monitor specimen temperature. Chromel-alumel thermocouples were inserted in shallow holes in the center and each end of the gage section of a dummy specimen and in each grip. In test configuration, with a slight load on the specimen, a plot of specimen temperature versus upper and lower grip and controller temperatures was developed over the range room temperature to 550° F. The upper grip was used to control the furnace temperature. During the actual testing the grip temperatures were used to obtain

desired specimen temperatures. Experiments indicated that this method is accurate to plus or minus 2° F.

The yield load, ultimate load, fracture load, total elongation, and uniform elongation were determined directly from the load-extension curve. The yield strength, ultimate strength, and fracture strength were calculated using the original cross-sectional area. The final diameter and final gage length were determined from post-fracture photographs. The fracture area used to calculate the fracture stress (true stress at fracture) and percent reduction in area was computed using the final diameter measurement.

5-2. CHARPY V-NOTCH IMPACT TEST RESULTS

The toughness results from Charpy V-notch impact tests performed on the various surveillance materials in Capsule D after irradiation to $2.22 \times 10^{19} n/cm^2$ are presented in Tables 5-1 through 5-3 and Figures 5-1 through 5-4. Instrumented Charpy impact test results for the various materials are shown in Tables 5-4 through 5-6. A summary of the surveillance test results is presented in Table 5-7. The fractured surfaces of the impact specimens are shown in Figures 5-5 through 5-8.

Irradiation of Charpy V-notch specimens from the intermediate shell course plate W9807-4 to $2.22 \times 10^{19} n/cm^2$ resulted in a 41-joule (30 ft. lb.) and 68-joule (50 ft. lb.) transition temperature increase of 43° C and 46° C respectively when compared with unirradiated values as shown in Figure 5-1. The upper shelf energy of plate W9807-4 decreased by 22-joule (16 ft. lb.). A comparison of these results with prior results from irradiations at lower fluences shown in Table 5-8 indicates that the increased neutron fluence produced no significant increase in transition temperature but did reduce the upper shelf energy level by approximately 18-joule.

Weld metal specimens irradiated to $2.22 \times 10^{19} n/cm^2$ resulted in a 41- and 68-joule transition temperature increase of 61° C and 72° C respectively and an upper shelf energy decrease of 30-joule when compared with unirradiated values as shown in Figure 5-2. A comparison of these results with prior test results on material irradiated to $2.39 \times 10^{18} n/cm^2$ is shown in Table 5-8. These results show that the transition temperature increases for the $2.22 \times 10^{19} n/cm^2$ irradiation were approximately 10° C higher than the results of irradiation at $2.39 \times 10^{18} n/cm^2$. In addition the higher irradiation fluence level appears to have produced a 9-joule recovery in upper shelf energy when compared with the lower fluence data.

Weld HAZ impact specimens irradiated to 2.22 x 10^{19}n/cm^2 showed a 41- and 68-joule transition temperature increase of 61° C and 56° C respectively when compared with unirradiated values as shown in Figure 5-3. No decrease in upper shelf energy resulted from the irradiation. A comparison of these results with prior tests results on material irradiated to 2.39 x 10^{18}n/cm^2 is shown in Table 5-8. The results indicate that irradiation to 2.22 x 10^{19}n/cm^2 produced an approximate 25° C additional increase in transition temperature but a significant improvement in upper shelf energy.

ASTM A302B correlation monitor material irradiated to 2.22 x 10^{19}n/cm^2 showed a 41- and 68-joule transition temperature increase of 78° C and 83° C respectively when compared with unirradiated results as shown in Figure 5-4. The upper shelf of the monitor material decreased by 23-joule. A comparison of these results with the results of tests at three lower neutron fluence levels is shown in Table 5-8. These results show that irradiation to 2.22 x 10^{19}n/cm^2 produces an approximate 25-30° C additional increase in transition temperature when compared with the results for the lowest level of irradiation (2.39 x 10^{18}n/cm^2).

The fracture appearance of each irradiated Charpy specimens from the various materials is shown in Figures 5-5 through 5-8. An increasing ductile or tougher appearance with increasing temperature can be noted for each of the materials.

Figure 5-9 shows a comparison of the 41-joule transition temperature increase for the Connecticut Yankee surveillance materials with predicted increases using the methods of NRC Regulatory Guide 1.99 Revision 1.

This comparison shows that all the materials exhibited 41-joule transition temperature increases lower than would be predicted for irradiations at 2.22 x 10^{19}n/cm^2. This behavior is consistent with the results from other reactor vessel surveillance capsules evaluated as part of this EPRI program. Based on the Connecticut Yankee surveillance capsule test results to date, it can be concluded that the reactor vessel beltline region material is not as sensitive to radiation as predicted and a saturation of radiation damage may be occurring.

5-3. TENSION TEST RESULTS

The results of tension tests performed on shell plate W9807-4 and weld metal are shown in Table 5-9 and Figures 5-10 and 5-11 respectively. An increase in 0.2% yield strength of approximately 80 and 110 MPa was exhibited by the plate and

weld metal respectively. These increases indicate that the weld metal is more sensitive to radiation than the base metal plate which is consistent with transition temperature increases observed for these materials. Photographs of the fractured tension specimens are shown in Figure 5-12. A typical stress strain curve for the tension tests is shown in Figure 5-13.

5-4. WEDGE OPENING LOADING TESTS

Wedge Opening Loading (WOL) fracture mechanics specimens which were contained in the surveillance capsule have been stored at the Westinghouse Research Laboratory; they will be tested and reported on later.

TABLE 5-1

CHARPY IMPACT DATA FOR CONNECTICUT YANKEE REACTOR VESSEL SHELL PLATE W9807-4 (IRRADIATED TO 2.22 x 10^{19} n/cm^2)

Sample No.	Temperature		Impact Energy		Lateral Expansion		Shear (%)
	(°C)	(°F)	(J)	(ft-lbs)	(mm)	(mils)	
Y48	-18	0	11.5	8.5	0.36	14.0	5
Y46	10	50	41.5	30.5	0.51	20.0	23
Y41	10	50	24.5	18.0	0.56	22.0	20
Y42	24	75	70.0	51.5	0.89	35.0	33
Y43	66	150	102.5	75.5	1.32	52.0	46
Y44	93	200	131.0	96.5	1.83	72.0	83
Y45	149	300	154.0	113.5	1.96	77.0	100
Y47	177	350	144.5	106.5	2.01	79.0	100

TABLE 5-2

CHARPY IMPACT DATA FOR CONNECTICUT YANKEE REACTOR VESSEL WELD METAL AND HAZ MATERIAL (IRRADIATED TO 2.22 x 10^{19} n/cm^2)

Sample No.	Temperature		Impact Energy		Lateral Expansion		Shear (%)
	(°C)	(°F)	(J)	(ft-lb)	(mm)	(mils)	
Weld Metal							
D15	-12	10	16.5	12.0	0.15	6.0	14
D9	16	60	40.5	30.0	0.56	22.0	39
D12	24	75	51.0	37.5	0.64	25.0	31
D14	38	100	54.0	40.0	0.79	31.0	57
D16	66	150	80.0	59.0	1.27	50.0	72
D11	93	200	93.5	69.0	1.40	55.0	97
D10	149	300	106.5	78.5	1.83	72.0	100
D13	204	400	119.5	88.0	1.78	70.0	100
HAZ Metal							
H15	-12	10	32.0	23.5	0.30	12.0	31
H11	24	75	36.0	26.5	0.51	20.0	38
H9	66	150	73.0	54.0	1.24	49.0	68
H10	66	150	42.5	31.5	1.02	40.0	46
H14	79	175	137.0	101.0	1.96	77.0	100
H16	93	200	133.0	98.0	1.74	68.5	100
H12	149	300	112.5	83.0	1.93	76.0	100
H13	204	400	119.5	88.0	1.84	72.5	100

TABLE 5-3

CHARPY IMPACT DATA FOR THE ASTM A302B CORRELATION MONITOR MATERIAL (IRRADIATED TO 2.22 x 10^{19} n/cm^2)

Sample No.	Temperature		Impact Energy		Lateral Expansion		Shear (%)
	(°C)	(°F)	(J)	(ft-lbs)	(mm)	(mils)	
R49	-12	10	4.0	3.0	0.30	12.0	1
R50	24	75	16.5	12.0	0.38	15.0	14
R53	71	160	37.5	27.5	0.61	24.0	27
R51	93	200	42.5	31.5	1.07	42.0	51
R54	107	225	76.0	56.0	1.04	41.0	93
R55	121	250	78.5	58.0	1.09	43.0	100
R52	149	300	84.5	62.5	1.14	45.0	100
R56	204	400	84.0	62.0	1.27	50.0	100

TABLE 5-4

INSTRUMENTED CHARPY IMPACT TEST RESULTS FOR THE CONNECTICUT YANKEE REACTOR VESSEL SHELL PLATE W9807-4

Sample No.	Test Temp (°C)	Charpy Energy (J)	Normalized Energies			Yield Load (N)	Time to Yield (μs)	Maximum Load (N)	Time to Maximum (μs)	Fracture Load (N)	Arrest Load (N)	Yield Stress (MPa)	Flow Stress (MPa)
			Charpy Ed/A (kJ/m²)	Maximum Em/A (kJ/m²)	Prop Ep/A (kJ/m²)								
Y48	-18	11.5	144	99	45	13600	105	15100	165	15100	800	699	737
Y41	10	24.5	305	169	136	14100	100	15400	235	15400	2600	724	757
Y46	10	41.5	517	435	82	15300	100	18700	475	18700	1200	787	875
Y42	24	70.0	873	714	159	14200	100	19000	760	19000	5000	728	852
Y43	66	102.5	1280	552	728	12500	100	17300	660	16700	8700	644	767
Y44	93	131.0	1635	542	1093	12100	95	17100	650	10600	7700	624	751
Y45	149	154.0	1924	528	1395	11000	115	16400	680			567	706
Y47	177	144.5	1805	574	1231	11000	95	16300	710			567	703

TABLE 5-5

INSTRUMENTED CHARPY IMPACT TEST RESULTS FOR CONNECTICUT YANKEE REACTOR VESSEL WELD AND HAZ METAL

Sample Number	Test Temp (°C)	Charpy Energy (J)	Normalized Energies			Yield Load (N)	Time to Yield (μs)	Maximum Load (N)	Time to Maximum (μs)	Fracture Load (N)	Arrest Load (N)	Yield Stress (MPa)	Flow Stress (MPa)
			Charpy Ed/A (kJ/m²)	Maximum Em/A (kJ/m²)	Prop Ep/A (kJ/m²)								
Weld Metal													
D15	-12	16.5	203	168	36	16900	110	17700	210	17600	0	869	891
D9	16	40.5	508	375	134	15000	115	18400	425	18400	4200	773	860
D12	24	51.0	636	486	150	15400	115	19200	525	18700	500	790	888
D14	38	54.0	678	431	247	15000	95	18700	465	18700	8800	774	867
D16	66	80.0	1000	415	585	13000	100	17100	505	15200	8600	670	775
D11	93	93.5	1169	424	745	13500	95	17100	500			697	789
D10	149	106.5	1330	437	894	12500	105	16900	530			644	756
D13	204	119.5	1491	498	993	12600	105	16700	605			646	752
HAZ Metal													
H15	-12	32.0	398	338	60	17100	125	19600	365	19600	3000	879	943
H11	24	36.0	449	286	163	18600	100	21600	285	21600	7900	957	1036
H10	66	42.5	534	251	282	12900	90	15700	325	15700	7500	665	736
H9	66	73.0	915	425	490	13500	100	17100	505	16700	10800	694	787
H14	79	137.0	1712	637	1074	14800	110	19000	675			760	870
H16	93	133.0	1661	621	1040	14600	100	18600	670			752	854
H12	149	112.5	1407	466	941	12300	115	16700	585			632	746
H13	204	119.5	1491	519	972	12000	115	16500	635			617	733

TABLE 5-6

INSTRUMENTED CHARPY IMPACT TEST RESULTS FOR THE ASTM CORRELATION MONITOR MATERIAL

Sample No.	Test Temp (°C)	Charpy Energy (J)	Normalized Energies			Yield Load (N)	Time to Yield (μs)	Maximum Load (N)	Time to Maximum (μs)	Fracture Load (N)	Arrest Load (N)	Yield Stress (MPa)	Flow Stress (MPa)
			Charpy Ed/A (kJ/m²)	Maximum Em/A (kJ/m²)	Prop Ep/A (kJ/m²)								
R49	-12	4.0	51	42	8			14500	90	14500	0		
R50	24	16.5	203	132	71	15000	115	16300	190	16300	300	772	806
R53	71	37.5	466	314	152	14300	100	18400	365	18400	2600	737	841
R51	93	42.5	534	288	245	14700	120	17800	360	17100	6000	757	835
R54	107	76.0	949	453	496	13300	105	18100	515	18100	11900	682	808
R55	121	78.5	983	373	610	13600	100	17500	435			700	801
R52	149	84.5	1059	366	693	12300	90	17100	440			635	758
R56	204	84.0	1051	363	688	12100	100	16700	450			625	742

TABLE 5-7

THE EFFECT OF 288° IRRADIATION TO 2.22 x 10^{19} n/cm^2 (E > 1.0 Mev) ON THE NOTCH TOUGHNESS PROPERTIES OF CONNECTICUT YANKEE REACTOR VESSEL MATERIALS

Material	Transition Temperature												Δ Transition Temperature						Average Energy Absorption at Full Shear					
	Unirradiated						Irradiated												Unirradiated		Irradiated		Δ Energy	
	50 ft lb 68 J		30 ft lb 41 J		35 mils .9 mm		50 ft lb 68 J		30 ft lb 41 J		35 mils .9 mm		50 ft lb 68 J		30 ft lb 41 J		35 mils .9 mm							
	(° C)	(° F)	(° C)	(° F)	(° C)	(° F)	(° C)	(° F)	(° C)	(° F)	(° C)	(° F)	(° C)	(° F)	(° C)	(° F)	(° C)	(° F)	(J)	(ft lb)	(J)	(ft lb)	(J)	(ft lb)
Plate W9807-4	-11	13	-31	-24	-17	2	35	95	12	54	36	97	46	82	43	78	53	95	171	126	149	110	22	16
Weld Metal	-23	-10	-46	-50	-32	-25	49	120	15	60	43	110	72	130	61	110	75	135	142	105	112	83	30	22
HAZ Metal	14	57	-15	5	-3	25	70	157	46	115	52	125	56	100	61	110	56	100	119	88	125	92	5[a]	4[a]
Correlation Monitor	24	75	4	40	9	49	107	225	82	180	87	189	83	150	78	140	78	140	106	78	83	61	23	17

a. Increase in energy

TABLE 5-8

SUMMARY OF CONNECTICUT YANKEE REACTOR VESSEL SURVEILLANCE CAPSULE CHARPY IMPACT TEST RESULTS

Material	Fluence [b] 10^{19} n/cm^2	68 J 50 ft lb Trans. Temp Increase		41 J 30 ft lb Trans. Temp Increase		Decrease In Upper Shelf Energy	
		(°C)	(°F)	(°C)	(°F)	(J)	(ft lb)
Plate W9807-2	.239	19	35	19	35	24	18
	.471	19	35	19	35	15	11
	1.58	25	45	32	57	7	5
Plate W9807-4	.471	42	75	44	80	3[a]	2[a]
	1.58	37	67	37	67	5	4
	2.22	46	82	43	78	22	16
Plate W9807-7	.471	25	45	28	50	16	12
	1.58	28	51	29	53	4	3
Weld Metal	.239	61	110	53	95	39	29
	2.22	72	130	61	110	30	22
HAZ Metal	.239	31	55	39	70	34	25
	2.22	56	100	61	110	5[a]	4[a]
Correlation Monitor	.239	58	105	47	85	14	10
	.471	67	120	44	80	23	17
	1.58	78	141	71	127	11	8
	2.22	83	150	78	140	23	17

a. Shelf Energy Increase

b. Fluence values based on updated dosimetry evaluations discussed in Section 6.

TABLE 5-9

TENSILE PROPERTIES FOR CONNECTICUT YANKEE REACTOR VESSEL
MATERIAL IRRADIATED TO 2.22 x 10^{19} n/cm^2

Sample No.	Material	Test Temp °C (°F)	Yield Strength MPa (ksi)	Ultimate Strength MPa (ksi)	Fracture Load N (kip)	Fracture Stress MPa (ksi)	Fracture Strength MPa (ksi)	Uniform Elongation (%)	Total Elongation (%)	Reduction in Area (%)
Y7	Plate W9807-4	93 (200)	474 (68.8)	604 (87.6)	12,900 (2.90)	1240 (180.6)	407 (59.1)	10.1	24.1	67
Y6	Plate W9807-4	288 (550)	442 (64.2)	618 (89.6)	15,800 (3.55)	880 (127.9)	499 (72.3)	11.2	17.2	43
D4	Weld Metal	93 (200)	551 (80.0)	632 (91.7)	14,000 (3.15)	1200 (173.6)	442 (64.2)	10.2	21.9	63
D3	Weld Metal	288 (550)	541 (78.4)	657 (95.2)	15,000 (3.38)	1250 (181.2)	474 (68.8)	11.1	21.3	62

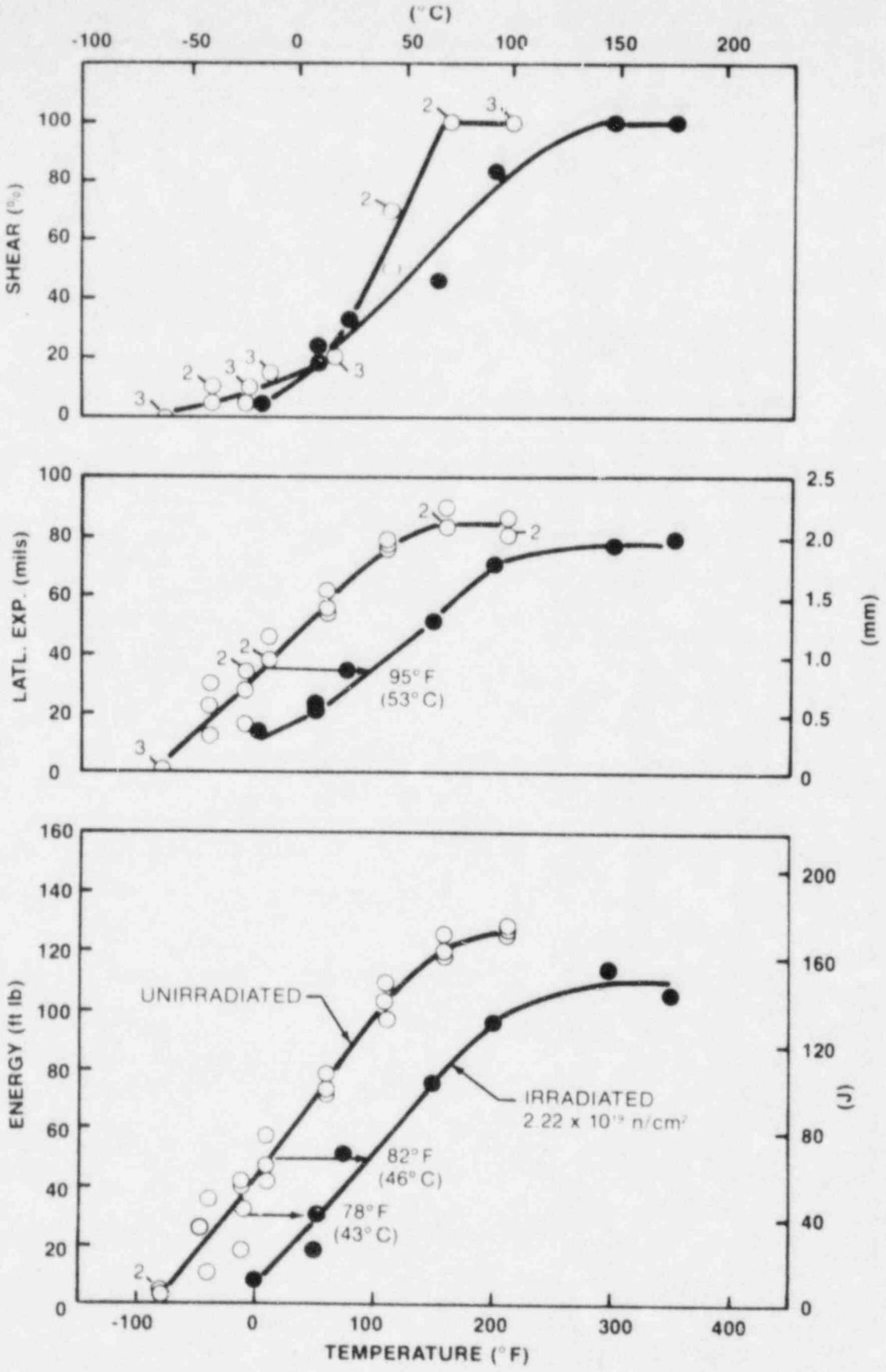

Figure 5-1. **Charpy V-Notch Impact Data for the Connecticut Yankee Reactor Vessel Shell Plate W9807-4.**

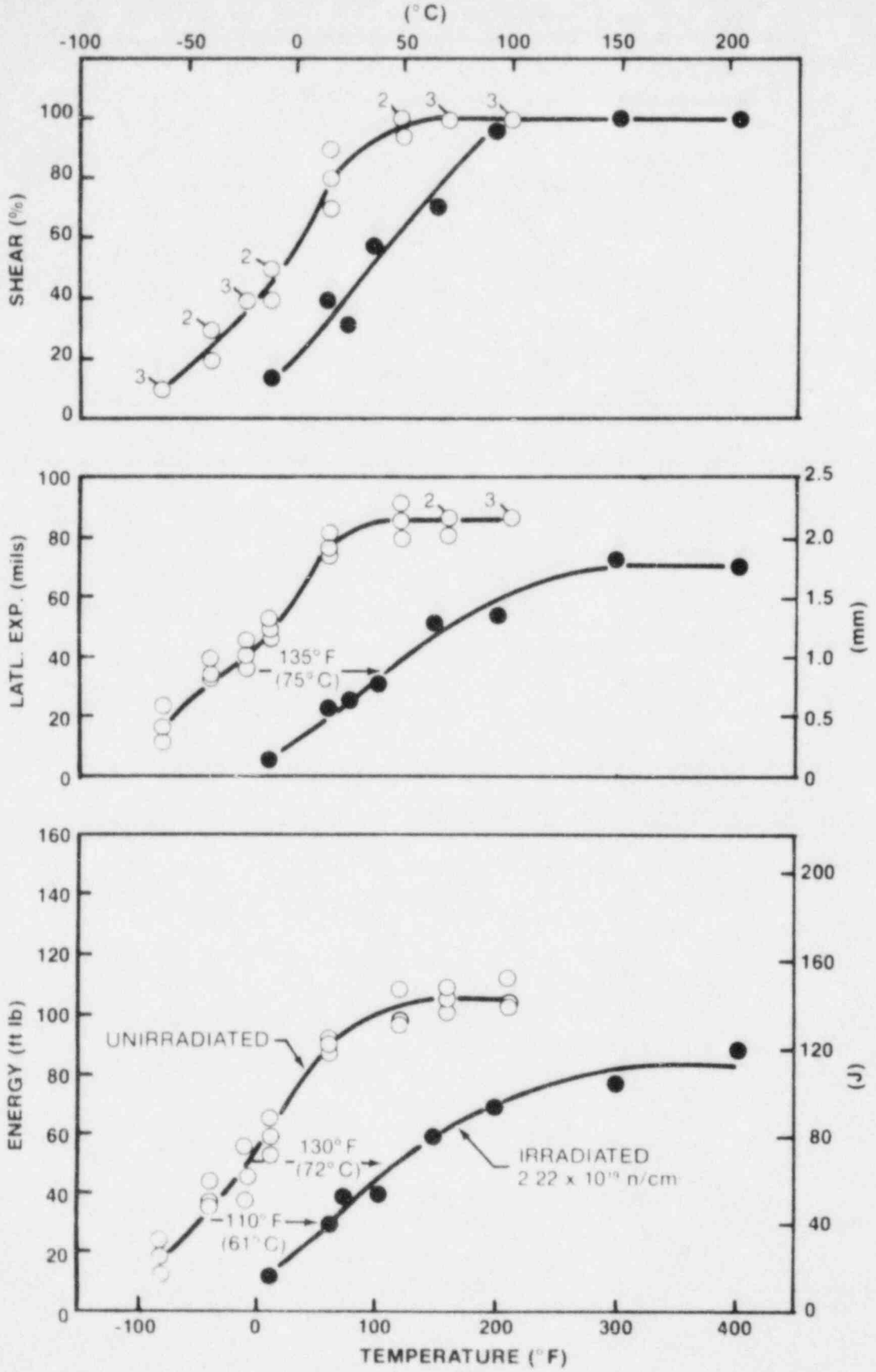

Figure 5-2. Charpy V-Notch Impact Data for the Connecticut Yankee Reactor Vessel Weld Metal.

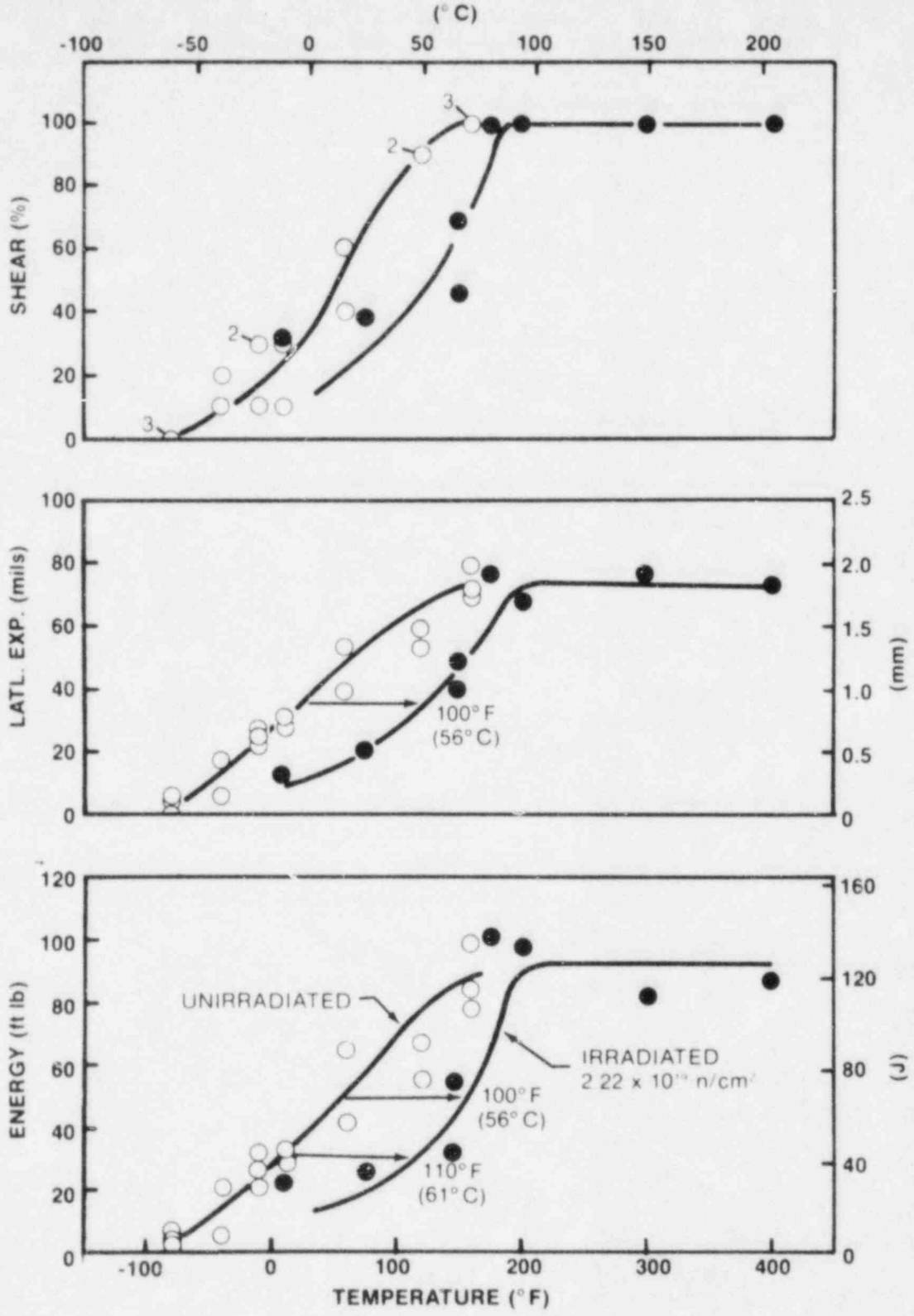

Figure 5-3. **Charpy V-Notch Impact Data for the Connecticut Yankee Reactor Vessel Weld Haz Material.**

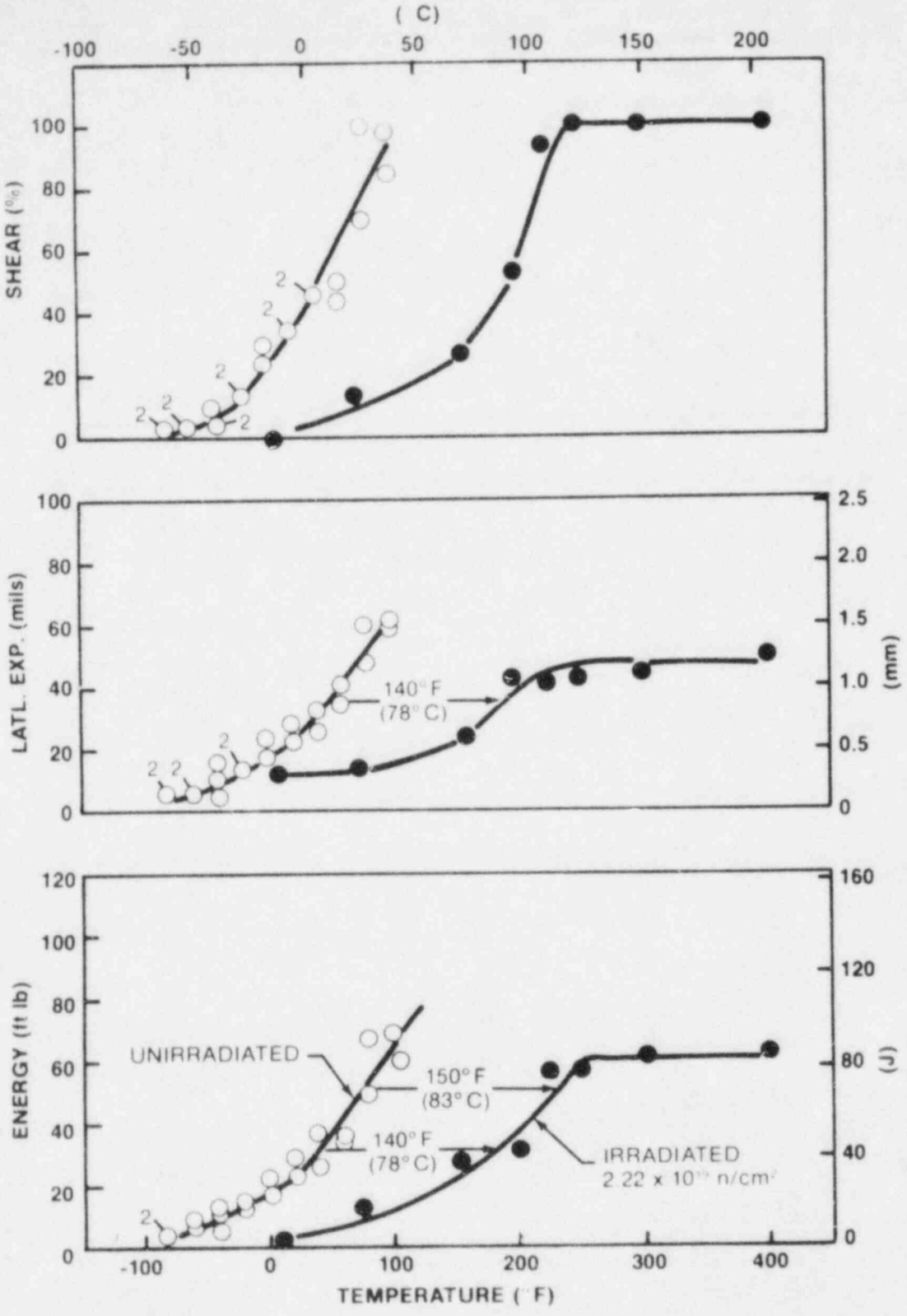

Figure 5-4. **Charpy V-Notch Impact Data for the Connecticut Yankee ASTM A302B Correlation Monitor Material.**

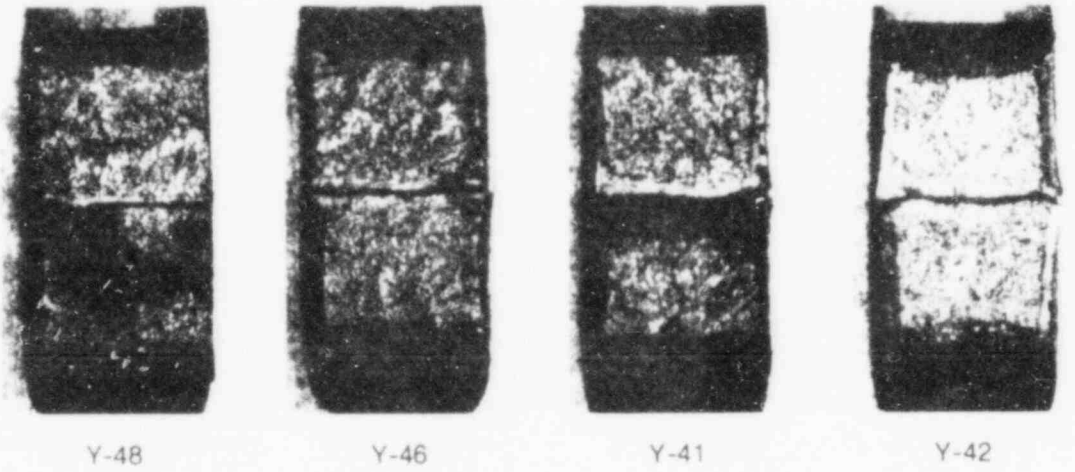

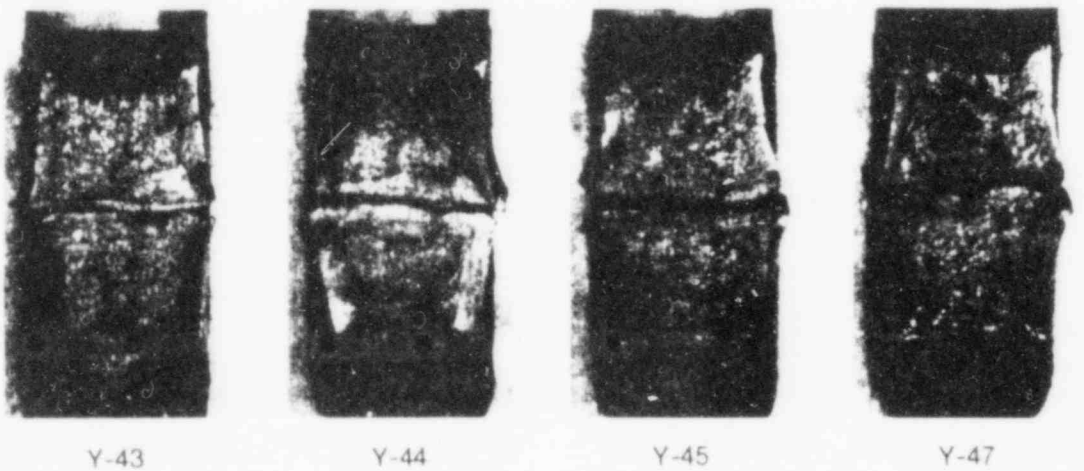

Figure 5-5. Charpy Impact Specimen Fracture Surfaces for the Connecticut Yankee Reactor Vessel Shell Plate W9807-4

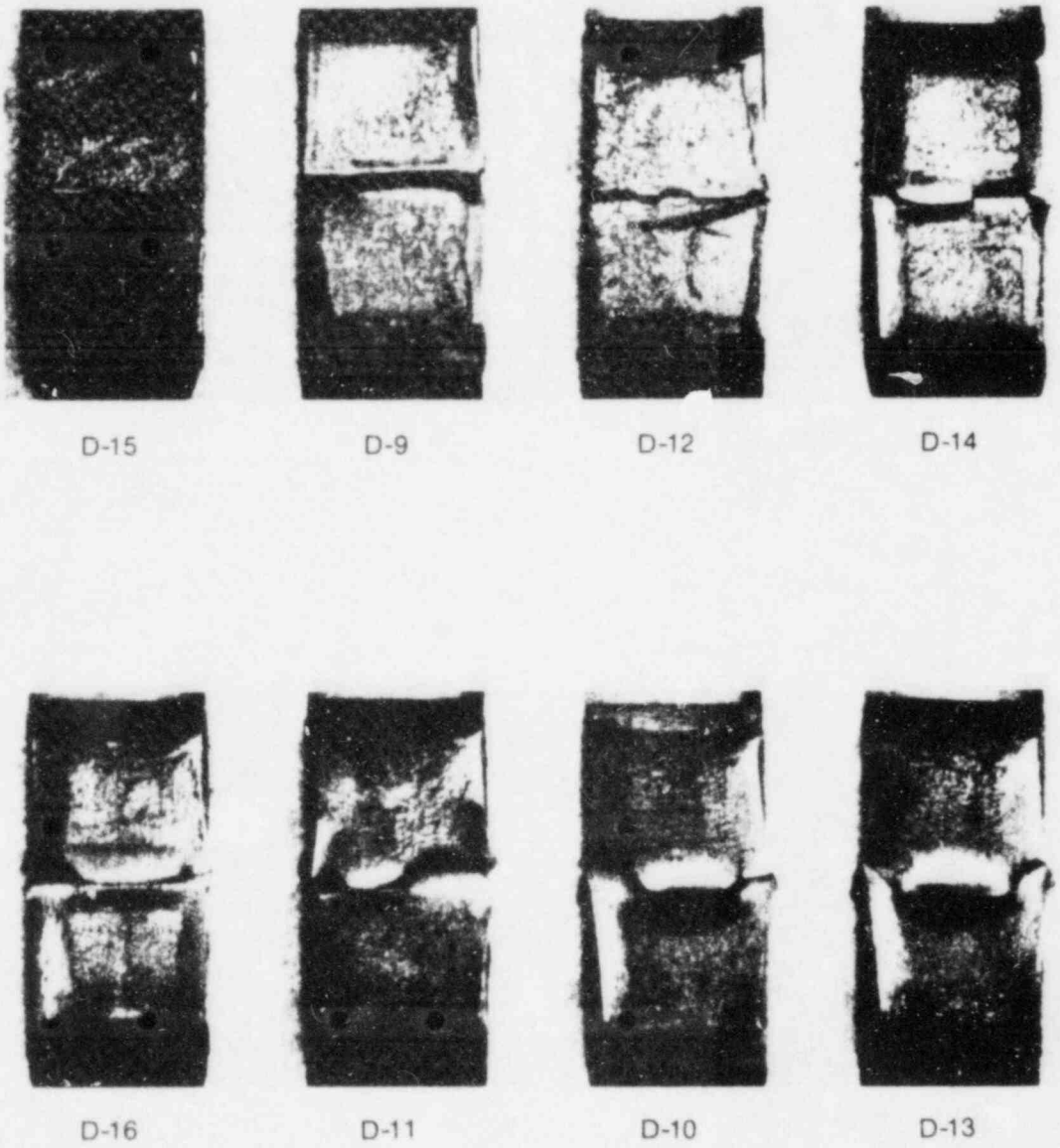

Figure 5-6. Charpy Impact Specimen Fracture Surfaces for the Connecticut Yankee Reactor Vessel Weld Metal

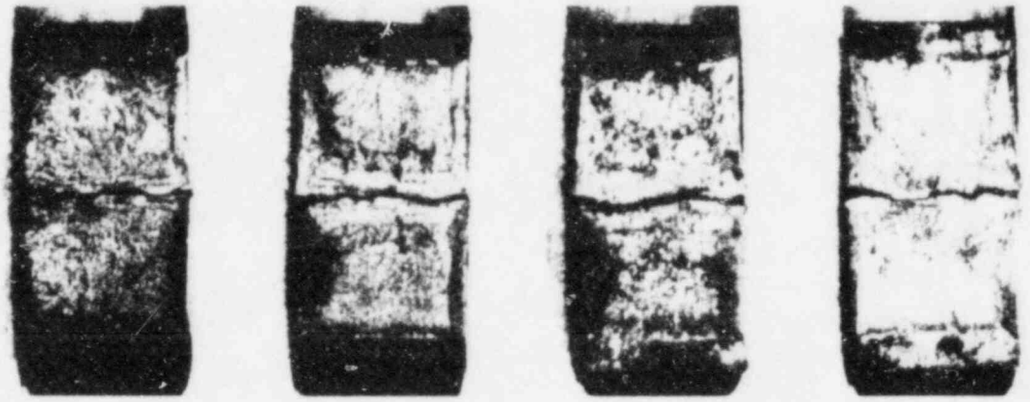

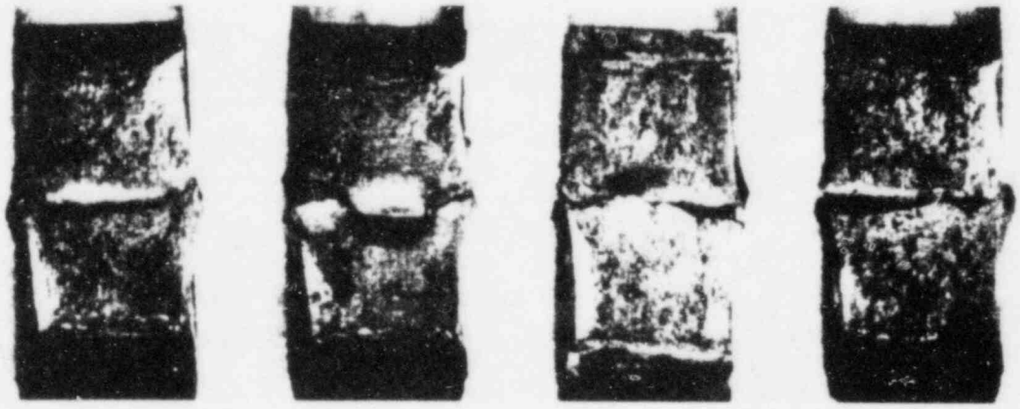

Figure 5-7. Charpy Impact Specimen Fracture Surfaces for the Connecticut Yankee Reactor Vessel Weld HAZ Metal

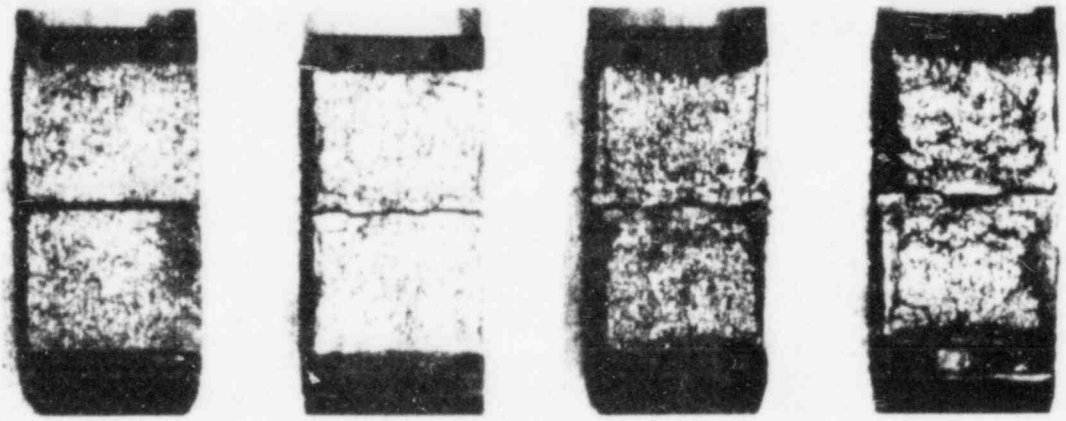

R-49 R-50 R-53 R-51

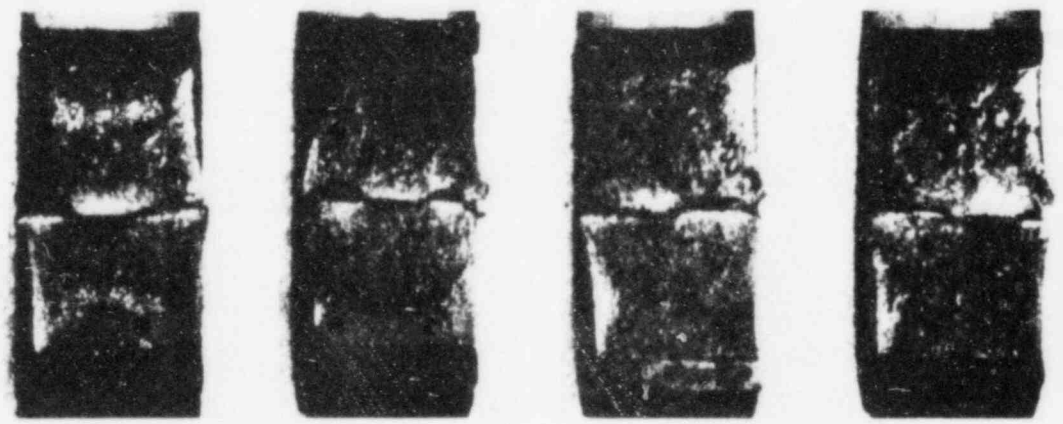

R-54 R-55 R-52 R-56

Figure 5-8. Charpy Impact Specimen Fracture Surfaces for the Connecticut Yankee ASTM A302B Correlation Monitor Material

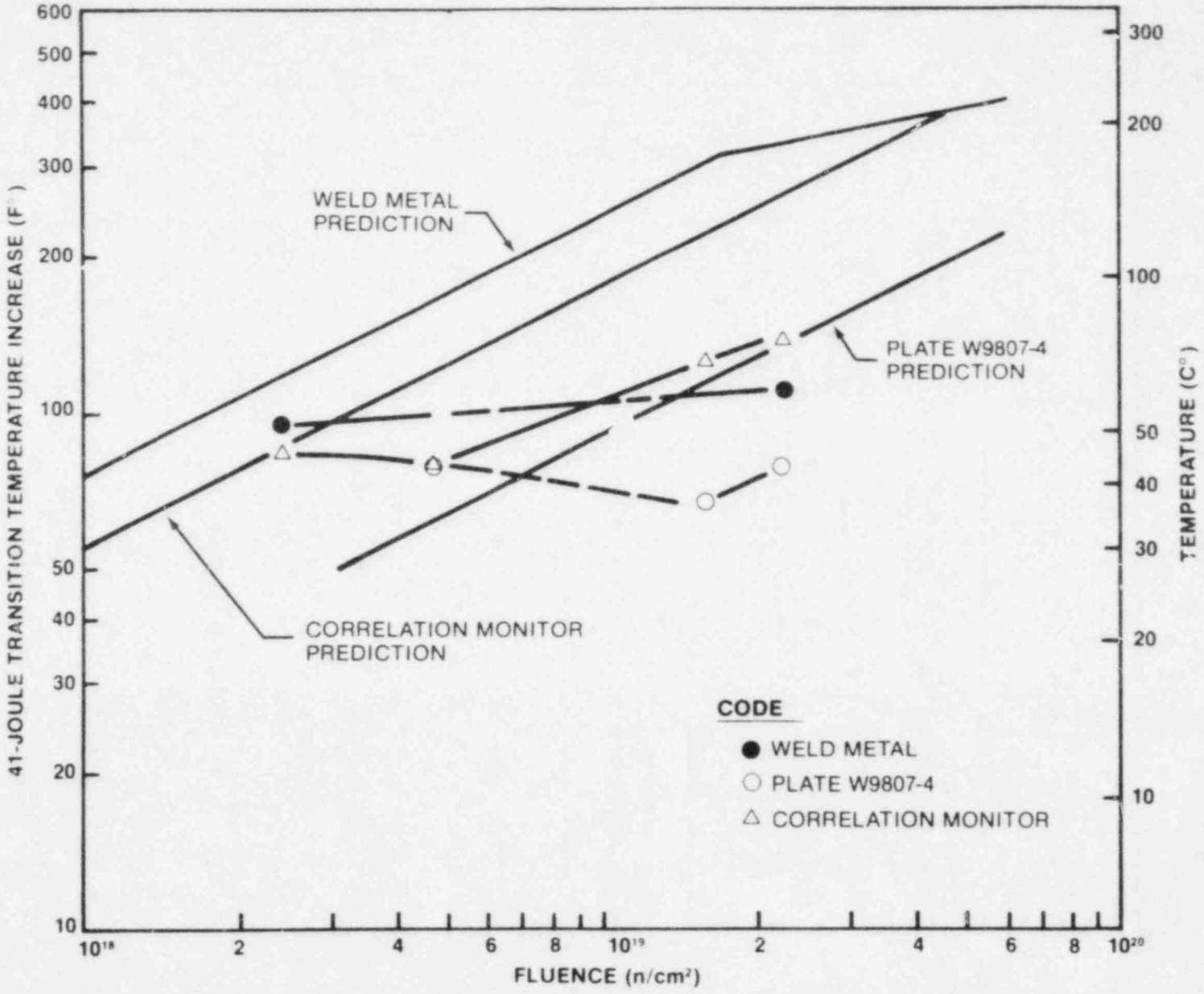

Figure 5-9. **Comparison of actual versus predicted 41-Joule transition temperature increases for Connecticut Yankee Reactor Vessel Materials. (Predicted increases based on NCR Regulatory Guide 1.99 Revision 1.)**

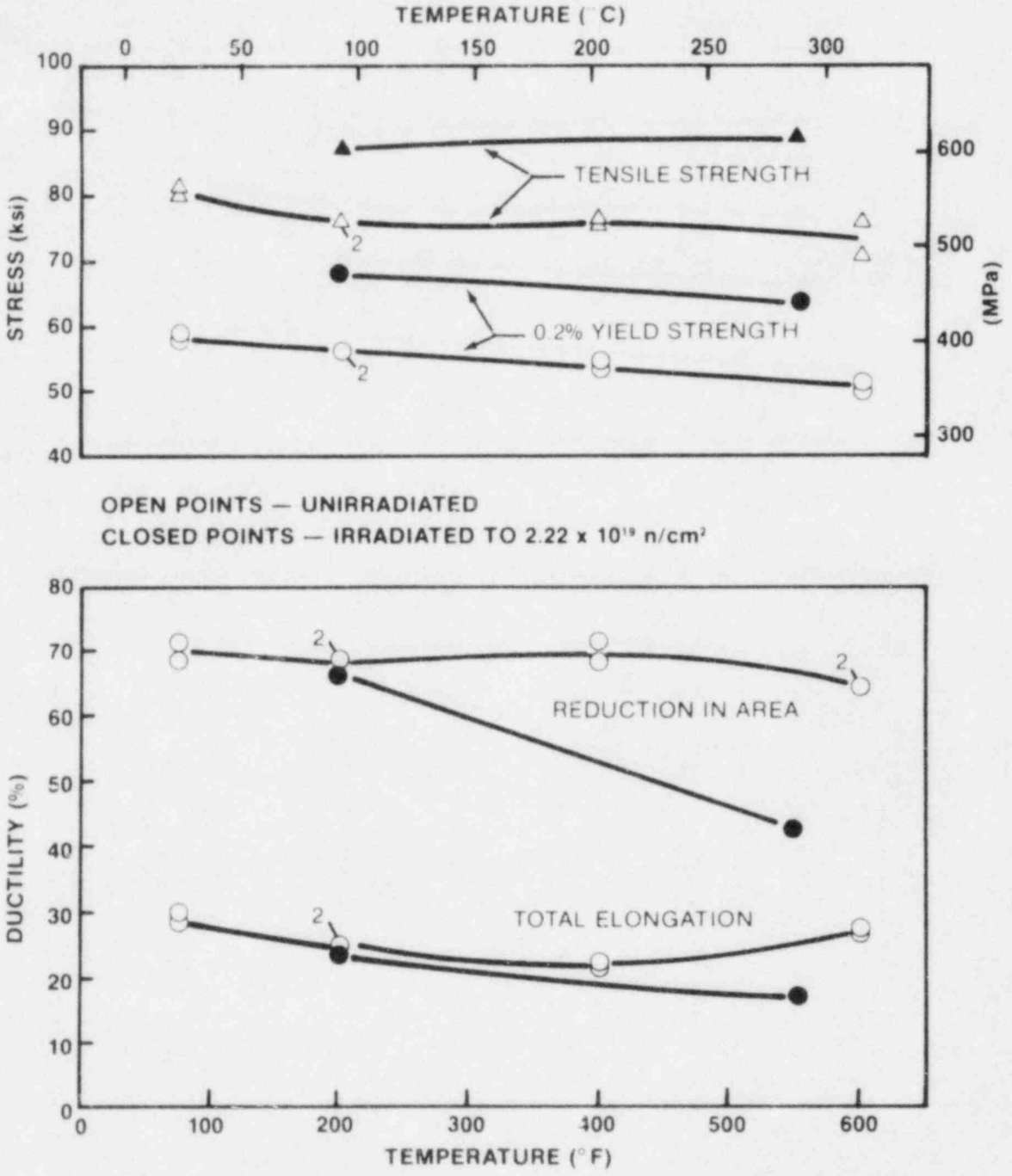

Figure 5-10 **Tensile Properties for Connecticut Yankee Reactor Vessel Shell Plate W9607-4.**

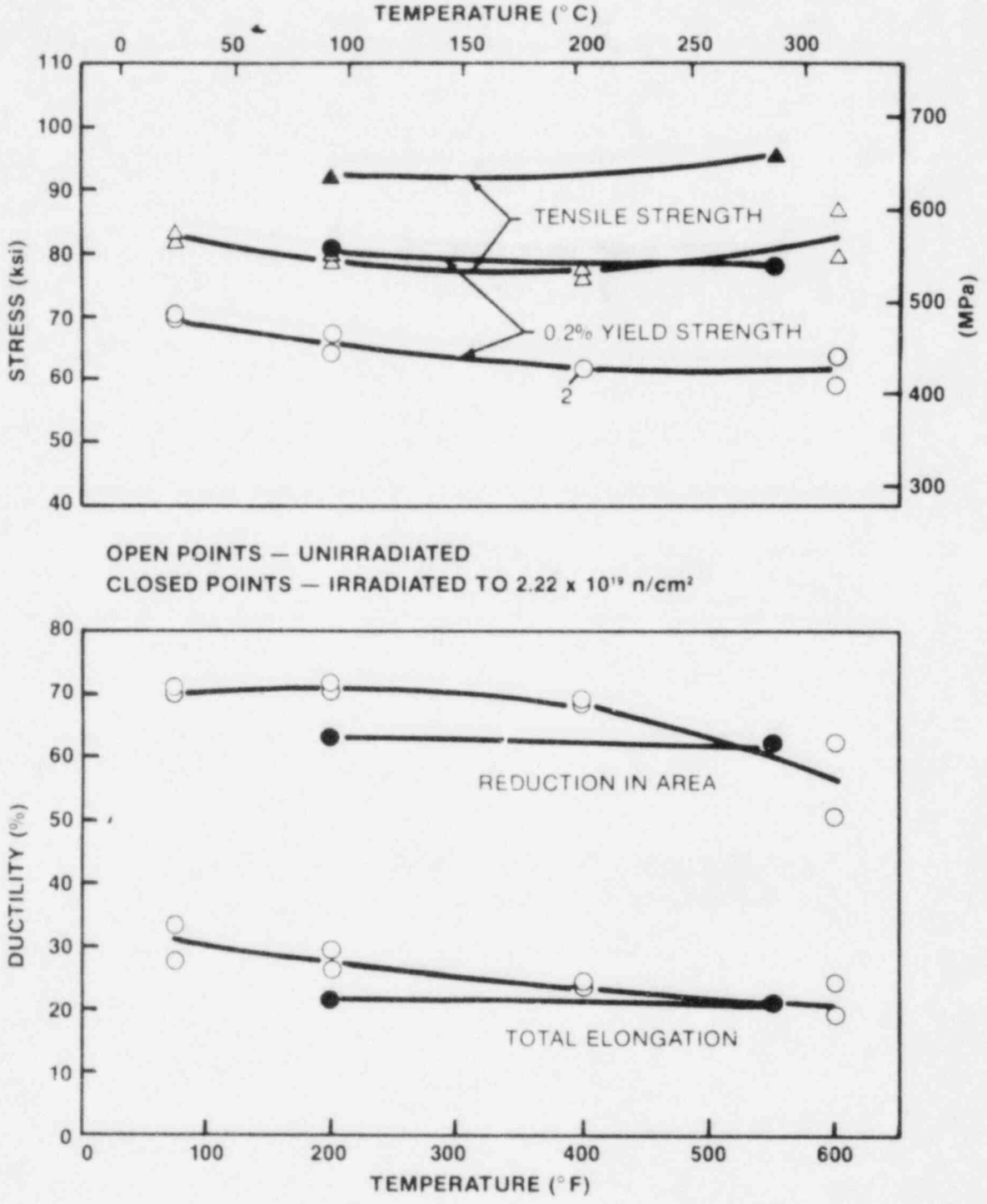

Figure 5-11. Tensile Properties for Connecticut Yankee Reactor Vessel Weld Metal.

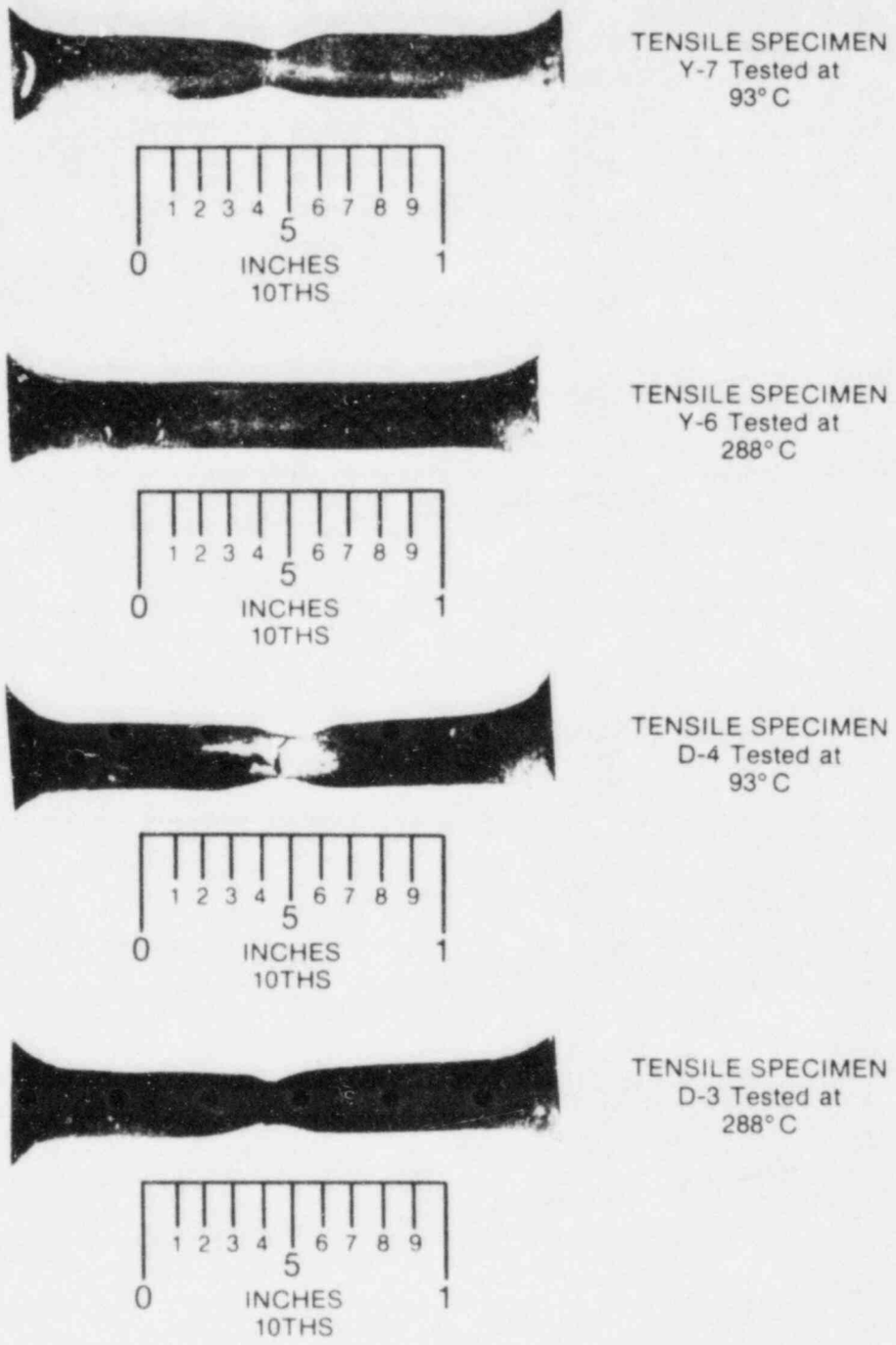

Figure 5-12. Fractured Tension Specimens From Connecticut Yankee Plate W9807-4 and Weld Metal

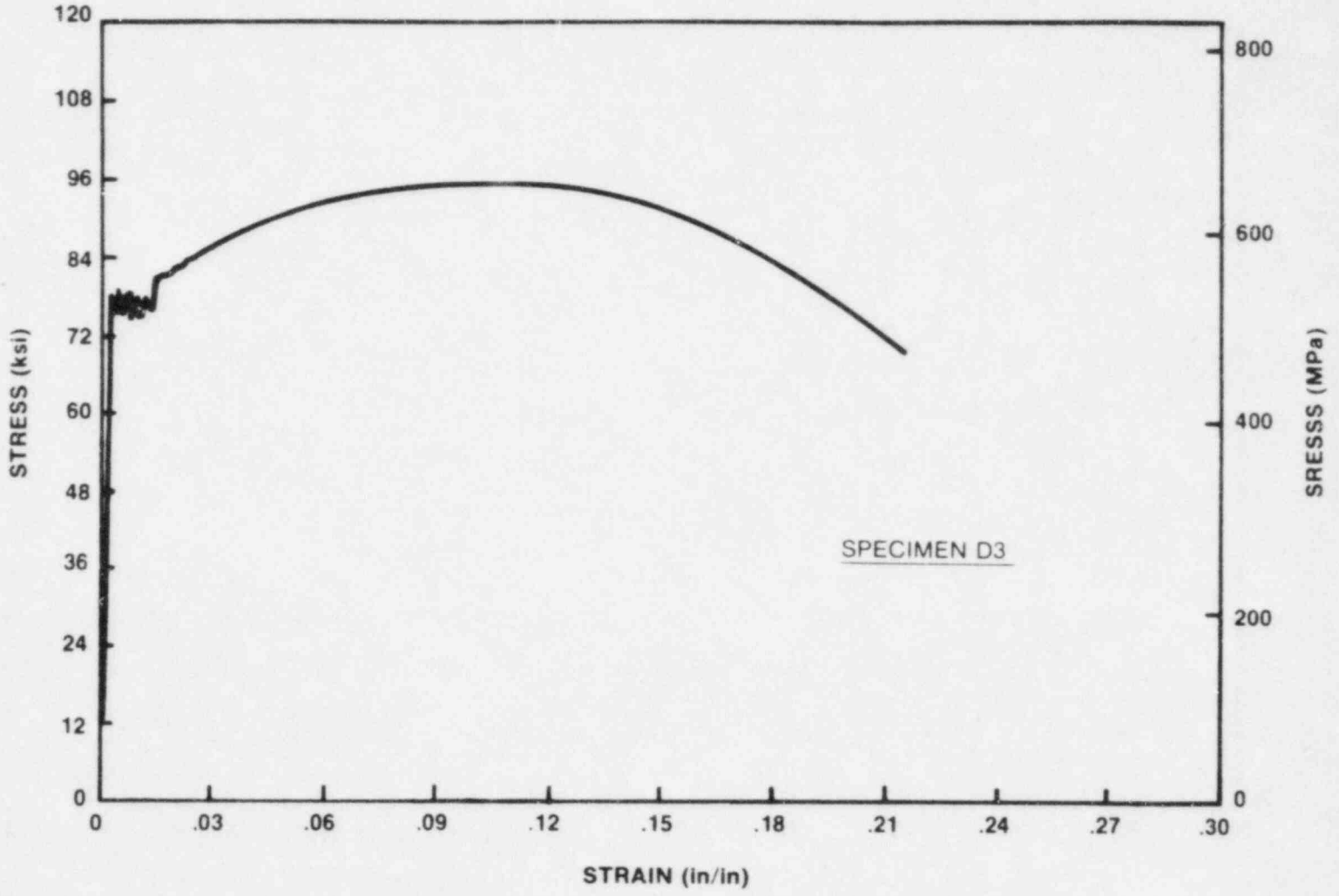

Figure 5-13. Typical stress strain curve for tension specimens.

SECTION 6
RADIATION ANALYSIS AND NEUTRON DOSIMETRY

6-1. INTRODUCTION

Knowledge of the neutron environment within the pressure vessel-surveillance capsule geometry is required as an integral part of LWR pressure vessel surveillance programs for two reasons. First, in the interpretation of radiation-induced property changes observed in materials test specimens, the neutron environment (fluence, flux) to which the test specimens were exposed must be known. Second, in relating the changes observed in the test specimens to the present and future condition of the reactor pressure vessel, a relationship between the environment at various positions within the reactor vessel and that experienced by the test specimens must be established. The former requirement is normally met by employing a combination of rigorous analytical techniques and measurements obtained with passive neutron flux monitors contained in each of the surveillance capsules. The latter information, on the other hand, is derived solely from analysis.

This section describes a discrete ordinates Sn transport analysis performed for the Connecticut Yankee reactor to determine the fast neutron ($E > 1.0$ Mev) flux and fluence as well as the neutron energy spectra within the reactor vessel and surveillance capsules; and, in turn, to develop lead factors for use in relating neutron exposure on the pressure vessel to that of the surveillance capsules. Based spectrum-averaged reaction cross sections derived from this calculation, the analysis of the neutron dosimetry contained in Capsule D is discussed and updated evaluations of dosimetry from Capsules A, F, and H are presented.

6-2. DISCRETE ORDINATES ANALYSIS

A plan view of the Connecticut Yankee reactor geometry at the core midplane is shown in Figure 6-1. Since the reactor exhibits 1/8th core symmetry only a 0°-45° sector is depicted.

Eight irradiation capsules attached to the thermal shield are included in the design to constitute the reactor vessel surveillance program. The eight capsules are located symmetrically at 43.5° from the cardinal axes as shown in Figure 6-1.

A plan view of a single surveillance capsule attached to the thermal shield is shown in Figure 6-2. The stainless steel specimen container is 1-inch square and approximately 36 inches in height. The containers are positioned axially such that the specimens are centered on the core midplane, thus spanning the central 3 feet of the 10-foot-high reactor core.

From a neutronic standpoint, the surveillance capsule structures are significant. Thus, in order to properly ascertain the neutron environment at the test specimen locations, the capsules themselves must be included in the analytical model. Use of at least a two-dimensional computation is, therefore, mandatory.

In the analysis of the neutron environment within the Connecticut Yankee reactor geometry, predictions of neutron flux magnitude and energy spectra were made with the DOT [5] two-dimensional discrete ordinates code. The radial and azimuthal distributions were obtained from an R, Θ computation wherein the geometry shown in Figures 6-1 and 6-2 was described in the analytical model. In addition to the R, Θ computation, a second calculation in R, Z geometry was also carried out to obtain relative axial variations of neutron flux throughout the geometry of interest. In the R, Z analysis the reactor core was treated as an equivalent volume cylinder and, of course, the surveillance capsules were not included in the model.

Both the R, Θ and the R, Z analyses employed 21 neutron energy groups, an S_8 angular quadrature, and a P_1 cross-section expansion. The cross sections were generated via the Westinghouse GAMB1T [6] code system with broad group processing by the APPROPOS [7] and ANISN [8] codes. The energy group structure used in the analysis is listed in Table 6-1.

A key input parameter in the analysis of the integrated fast neutron exposure of the reactor vessel is the core power distribution. For this analysis, power distributions representative of time-averaged conditions derived from statistical studies of long-term operation of Westinghouse plants were employed. These input distributions include rod-by-rod spatial variations for all peripheral fuel assemblies.

It should be noted that this particular power distribution is intended to produce accurate end-of-life neutron exposure levels for the pressure vessel. As such, the calculation is indeed representative of an average neutron flux and deviations from cycle to cycle are to be expected.

TABLE 6-1

21 GROUP ENERGY STRUCTURE

Group No.	Lower Energy (Mev)
1	7.79*
2	6.07
3	4.72
4	3.68
5	2.87
6	2.23
7	1.74
8	1.35
9	1.05
10	0.821
11	0.388
12	0.111
13	4.09×10^{-2}
14	1.50×10^{-2}
15	5.53×10^{-3}
16	5.83×10^{-4}
17	7.89×10^{-5}
18	1.07×10^{-5}
19	1.86×10^{-6}
20	3.00×10^{-7}
21	0.00

*The upper energy of group 1 is 10.0 Mev

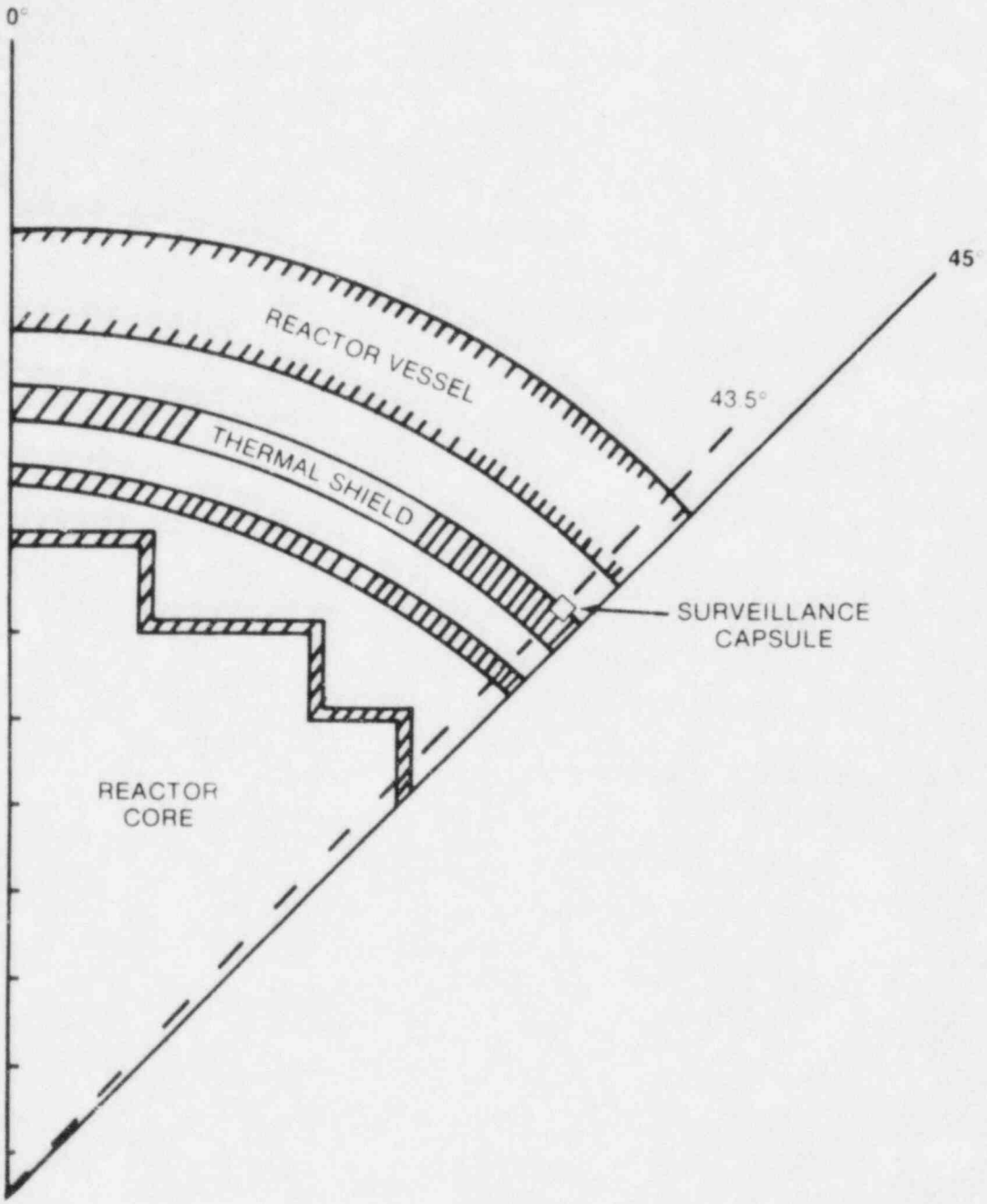

FIGURE 6-1. R, Theta Reactor Geometry

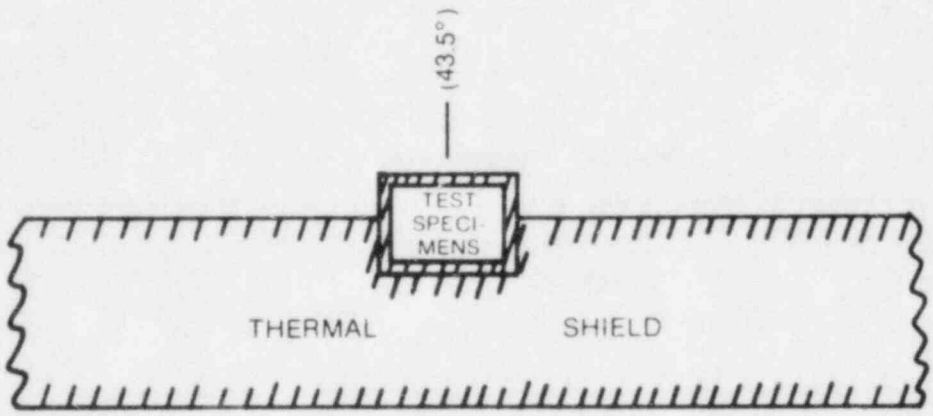

Figure 6-2. Surveillance Capsule Geometry

Having the results of the R, Θ and R, Z calculations, three-dimensional variations of neutron flux may be approximated by assuming that the following relation holds for the applicable regions of the reactor.

$$\phi(R,Z,\Theta E_g) = \phi(R,\Theta,E_g)\, F(Z,E_g) \qquad (6\text{-}1)$$

where:

$\phi(R,Z,\Theta E_g)$ = neutron flux at point R,Z,Θ within energy group g

$\phi(R,\Theta,E_g)$ = neutron flux at point R,Θ within energy group g obtained from the R,Θ calculation

$F(Z,E_g)$ = relative axial distribution of neutron flux within energy group g obtained from the R,Z calculation

6-3. NEUTRON DOSIMETRY

The passive neutron flux monitors included in the Connecticut Yankee surveillance program are listed in Table 6-2. The first five reactions in Table 6-2 are used as fast neutron monitors to relate neutron fluence ($E > 1.0$ Mev) to measured materials properties changes. To properly account for burnout of the product isotope generated by fast neutron reactions, it is necessary to also determine the magnitude of the thermal neutron flux at the monitor location. Therefore, bare and cadmium-covered cobalt-aluminum monitors were also included.

The relative locations of the various monitors within the surveillance capsules are shown in Figure 4-2. The nickel, copper, and cobalt-aluminum monitors, in wire form, are placed in holes drilled in spacers at several axial levels within the capsules. In addition several iron dosimeters are obtained by removing samples from selected charpy specimens included in the test matrix. The cd-shielded neptunium and uranium fission monitors are accommodated within the dosimeter block located near the center of the capsule.

The use of the passive monitors such as those listed in Table 6-2 does not yield a direct measure of the energy-dependent flux level at the point of interest. Rather, the activation or fission process is a measure of the integrated effect that the time- and energy-dependent neutron flux has on the target material over the course of

the irradiation period. An accurate assessment of the average neutron flux level incident on the various monitors may be derived from the activation measurements only if the irradiation parameters are well known. In particular, the following variables are of interest:

TABLE 6-2

NUCLEAR CONSTANTS FOR NEUTRON FLUX MONITORS CONTAINED IN SURVEILLANCE CAPSULES

Monitor Material	Reaction of Interest	Target Weight Fraction	Product Half-Life	Fission Yield (%)
Copper	Cu^{63} (n, α) Co^{60}	0.6917	5.27 Yrs	
Iron	Fe^{54} (n, p) Mn^{54}	0.0585	314 Dys	
Nickel	Ni^{58} (n, p) Co^{58}	0.6777	71.4 Dys	
Uranium-238*	U^{238} (n, f) Cs^{137}	1.0	30.2 Yrs	6.3
Neptunium-237*	Np^{237} (n, f) Cs^{137}	1.0	30.2 Yrs	6.5
Cobalt-Aluminum*	Co^{59} (n, γ) Co^{60}	0.0015	5.27 Yrs	
Cobalt-Aluminum	Co^{59} (n, γ) Co^{60}	0.0015	5.27 Yrs	

*Denotes that monitor is Cadmium shielded.

- The operating history of the reactor
- The energy response of the monitor
- The neutron energy spectrum at the monitor location
- The physical characteristics of the monitor

The analysis of the passive monitors and subsequent derivation of the average neutron flux requires completion of two procedures. First, the disintegration rate of product isotope per unit mass of monitor must be determined. Second, in order to define a suitable spectrum averaged reaction cross section, the neutron energy spectrum at the monitor location must be calculated.

The specific activity of each of the monitors is determined using established ASTM procedures.[9, 10, 11, 12, 13] Following sample preparation, the activity of each monitor is determined by means of a lithium-drifted germanium, Ge(Li), gamma spectrometer. The overall standard deviation of the measured data is a function of the precision of sample weighing, the uncertainty in counting, and the acceptable error in detector calibration. For the samples removed from Connecticut Yankee, the overall 2σ deviation in the measured data is determined to be $\pm$ 10 percent. The neutron energy spectra are determined analytically using the method described in Section 6-1.

Having the measured activity of the monitors and the neutron energy spectra at the locations of interest, the calculation of the neutron flux proceeds as follows.

The reaction product activity in the monitor is expressed as

$$R = \frac{N_o}{A} f_i Y \int_E \sigma(E)\phi(E) \sum_{j=1}^{N} \frac{P_j}{P_{max}} (1 - e^{-\lambda t_j}) e^{-\lambda t_d} \qquad (6\text{-}2)$$

where:

R = induced product activity

N_o = Avagadro's number

A = atomic weight of the target isotope

f_i = weight fraction of the target isotope in the target material

Y = number of product atoms produced per reaction

$\sigma(E)$ = energy-dependent reaction cross section

$\phi(E)$ = energy-dependent neutron flux at the monitor location with the reactor at full power

P_j = average core power level during irradiation period j

P_{max} = maximum or reference core power level

λ = decay constant of the product isotope

t_j = length of irradiation period j

t_d = decay time following irradiation period j

Since neutron flux distributions are calculated using multigroup transport methods and, further, since the prime interest is in the fast neutron flux above 1.0 Mev, spectrum-averaged reaction cross sections are defined such that the integral term in equation (6-2) is replaced by the following relation.

$$\int_E \sigma(E)\ \phi(E)dE = \bar{\sigma}\,\phi(E > 1.0\ \text{Mev})$$

where:

$$\bar{\sigma} = \frac{\int_0^{\infty} \sigma(E)\,\phi(E)\,dE}{\int_{1.0\,Mev}^{\infty} \phi(E)\,dE} = \frac{\sum_{G=1}^{N} \sigma_g \phi_g}{\sum_{G=G_{1.0\,Mev}}^{N} \phi_g}$$

Thus, equation (6-2) is rewritten

$$R = \frac{N_o}{A} f_1 \gamma \bar{\sigma}\, \phi(E > 1.0\,Mev) \sum_{j=1}^{N} \frac{P_j}{P_{max}} (1-e^{-\lambda t_j})\, e^{-\lambda t_d}$$

or, solving for the neutron flux,

$$\phi(E > 1.0\,Mev) = \frac{R}{\frac{N_o}{A} f_1 \gamma \bar{\sigma} \sum_{j=1}^{N} \frac{P_j}{P_{max}} (1-e^{-\lambda t_j})\, e^{-\lambda t_d}} \qquad (6\text{-}3)$$

The total fluence above 1.0 Mev is then given by

$$\Phi(E > 1.0\,Mev) = \phi(E > 1.0\,Mev) \sum_{j=1}^{N} \frac{P_j}{P_{max}} t_j \qquad (6\text{-}4)$$

where:

$$\sum_{j=1}^{N} \frac{P_j}{P_{max}} t_j$$ = total effective full power seconds of reactor operation up to the time of capsule removal

An assessment of the thermal neutron flux levels within the surveillance capsules is obtained from the bare and cadmium-covered $Co^{59}(n,\delta)Co^{60}$ data by means of cadmium ratios and the use of a 37-barn 2200 m/sec cross section. Thus,

$$\Phi_{Th} = \frac{R_{bare} \left\{ \frac{D-1}{D} \right\}}{\frac{N_o}{A} f_i \gamma \sigma \sum_{j=1}^{N} \frac{P_j}{P_{max}} (1-e^{-\lambda t_j}) e^{-\lambda t_d}} \quad (6\text{-}5)$$

where:

D is defined as $\frac{R_{bare}}{R_{Cd\ covered}}$

6-4. TRANSPORT ANALYSIS RESULTS

Results of the S_n transport calculations for the Connecticut Yankee reactor are summarized in Figures 6-3 through 6-7 and in Tables 6-3 through 6-5. In Figure 6-3, the calculated maximum neutron flux levels at the surveillance capsule centerline, pressure vessel inner radius, 1/4 thickness location, and 3/4 thickness location are presented as a function of azimuthal angle. In Figure 6-4, the radial distribution of maximum fast neutron flux ($E > 1.0$ Mev) through the thickness of the reactor pressure vessel is shown. The relative axial variation of neutron flux within the vessel is given in Figure 6-5. Absolute axial variations of fast neutron flux may be obtained by multiplying the levels given in Figures 6-3 or 6-4 by the appropriate values from Figure 6-5.

In Figure 6-6 the radial variations of fast neutron flux within each of the surveillance capsules is presented. These data, in conjunction with the maximum vessel flux,

are used to develop lead factors for each of the capsules. Here the lead factor is defined as the ratio of the fast neutron flux ($E > 1.0$ Mev) at the dosimeter block location (capsule center) to the maximum fast neutron flux at the pressure vessel inner radius. Updated lead factors for the Connecticut Yankee surveillance capsules are listed in Table 6-3. The lead factors presented in Table 6-3 differ from those previously published in reference 4 because of an improved neutron transport methodology which takes into account neutron flux perturbations introduced by the surveillance capsules and their associated structure.

Since the neutron flux monitors contained within the surveillance capsules are not all located at the same radial location, the measured disintegration rates are analytically adjusted for the gradients that exist within the capsules so that flux and fluence levels may be derived on a common basis at a common location. This point of comparison was chosen to be the capsule center. Analytically determined reaction rate gradients for use in the adjustment procedures are shown in Figure 6-7. All of the applicable fast neutron reactions are included.

In order to derive neutron flux and fluence levels from the measured disintegration rates, suitable spectrum-averaged reaction cross sections are required. The neutron energy spectrum calculated to exist at the center of each of the surveillance capsules is given in Table 6-4. The associated spectrum-averaged cross sections for each of the five fast neutron reactions are given in Table 6-5.

TABLE 6-3

CALCULATED FAST NEUTRON FLUX (E > 1.0 Mev) AND LEAD FACTORS FOR THE CONNECTICUT YANKEE SURVEILLANCE CAPSULES

Capsule Identification	Azimuthal Location	ϕ (E > 1.0 Mev) (n/cm²-sec)	Lead Factor
A	43.5°	7.20×10^{10}	0.97
F	43.5°	7.20×10^{10}	0.97
H	43.5°	7.20×10^{10}	0.97
D	43.5°	7.20×10^{10}	0.97
E	43.5°	7.20×10^{10}	0.97
B	43.5°	7.20×10^{10}	0.97
C	43.5°	7.20×10^{10}	0.97
G	43.5°	7.20×10^{10}	0.97

TABLE 6-4

CALCULATED NEUTRON ENERGY SPECTRUM AT THE CENTER OF THE CONNECTICUT YANKEE SURVEILLANCE CAPSULES

Group No.	Neutron Flux (n/cm^2-sec)
1	6.18×10^{8}
2	2.07×10^{9}
3	3.02×10^{9}
4	2.92×10^{9}
5	4.56×10^{9}
6	8.71×10^{9}
7	1.20×10^{10}
8	1.64×10^{10}
9	2.17×10^{10}
10	2.32×10^{10}
11	7.52×10^{10}
12	8.93×10^{10}
13	3.51×10^{10}
14	2.42×10^{10}
15	1.81×10^{10}
16	4.35×10^{10}
17	3.06×10^{10}
18	3.21×10^{10}
19	2.38×10^{10}
20	2.37×10^{10}
21	6.70×10^{10}

TABLE 6-5

SPECTRUM AVERAGED REACTION CROSS-SECTIONS AT THE CENTER OF THE CONNECTICUT YANKEE SURVEILLANCE CAPSULES

Reaction	$\bar{\sigma}$ (barns)
Fe^{54} (n, ρ) Mn^{54}	0.0750
Ni^{58} (n, ρ) Co^{58}	0.0986
Cu^{63} (n, α) Co^{60}	0.000618
U^{238} (n, f) Cs^{137}	0.351
Np^{237} (n, f) Cs^{137}	2.81

$$\bar{\sigma} = \frac{\int_{o}^{\infty} \sigma(E)\phi(E)dE}{\int_{1.0\ Mev}^{\infty} \phi(E)dE}$$

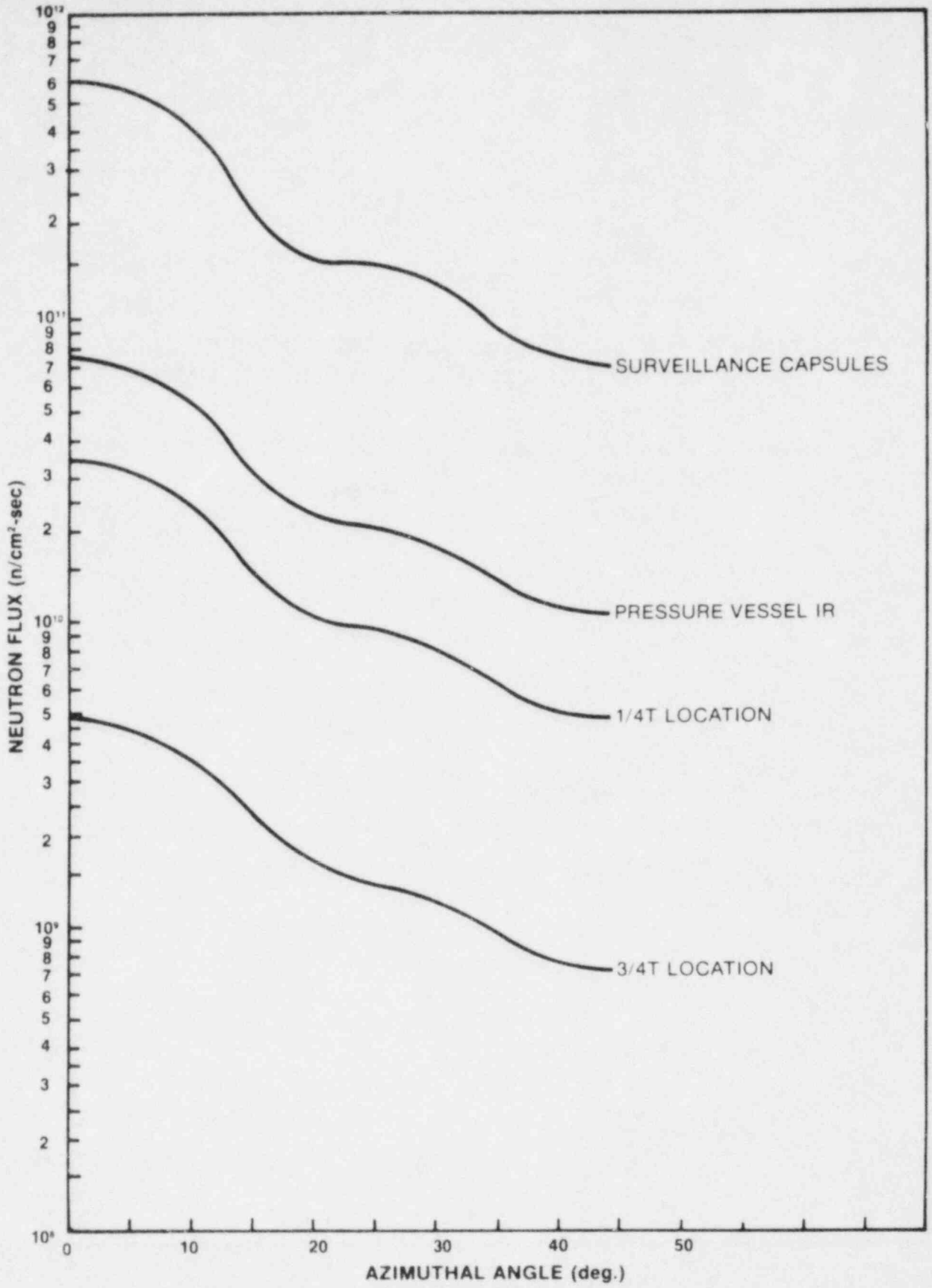

Figure 6-3. Calculated Azimuthal Distribution of Maximum Fast Neutron Flux (E > 1.0 Mev) within the Pressure Vessel — Surveillance Capsule Geometry.

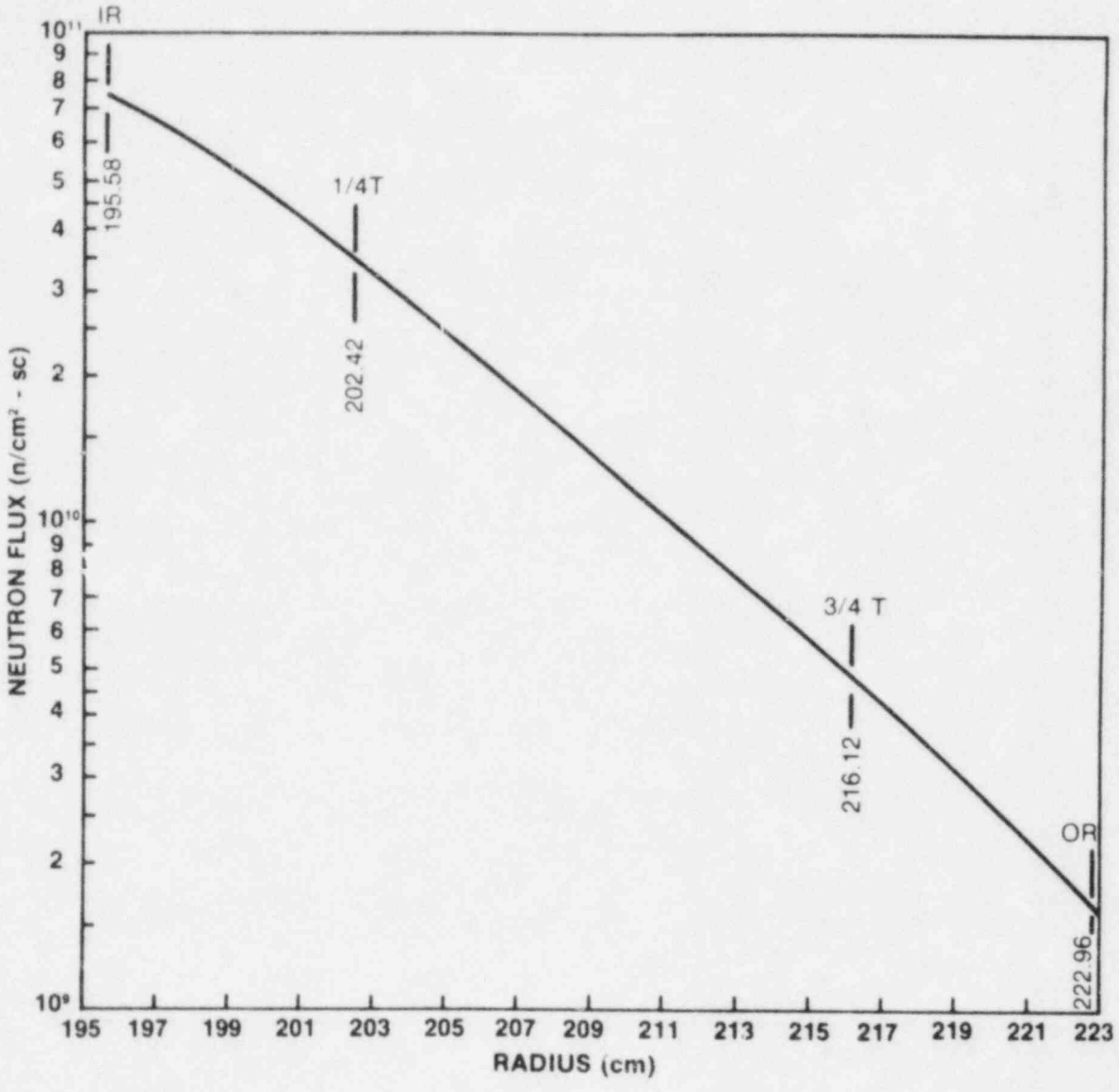

Figure 6-4. Calculated radial distribution of Maximum Fast Neutron Flux ($E > 1.0$ Mev) within the pressure vessel.

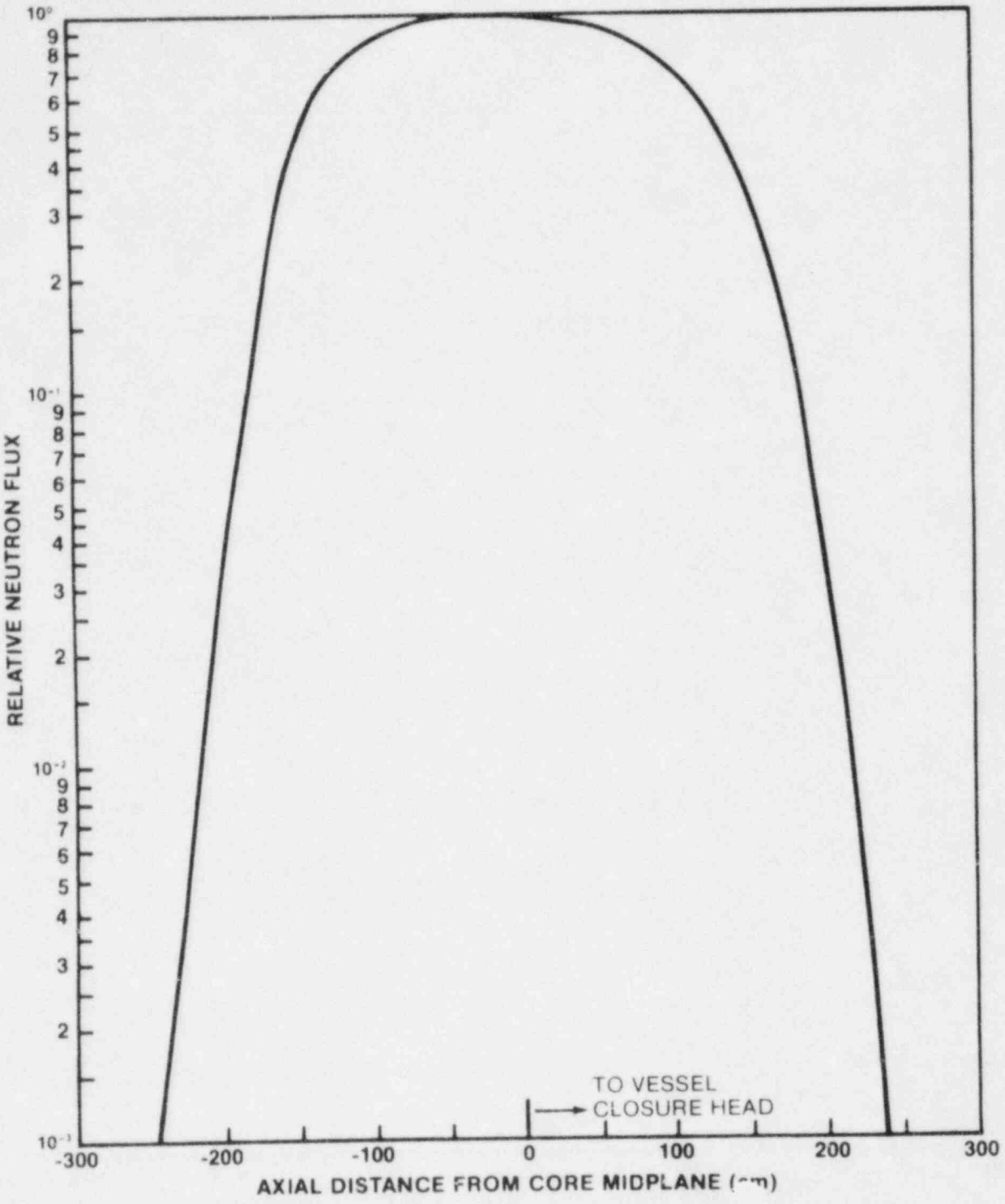

Figure 6-5. Relative axial variation of Fast Neutron Flux (E > 1.0 Mev) within the Pressure Vessel.

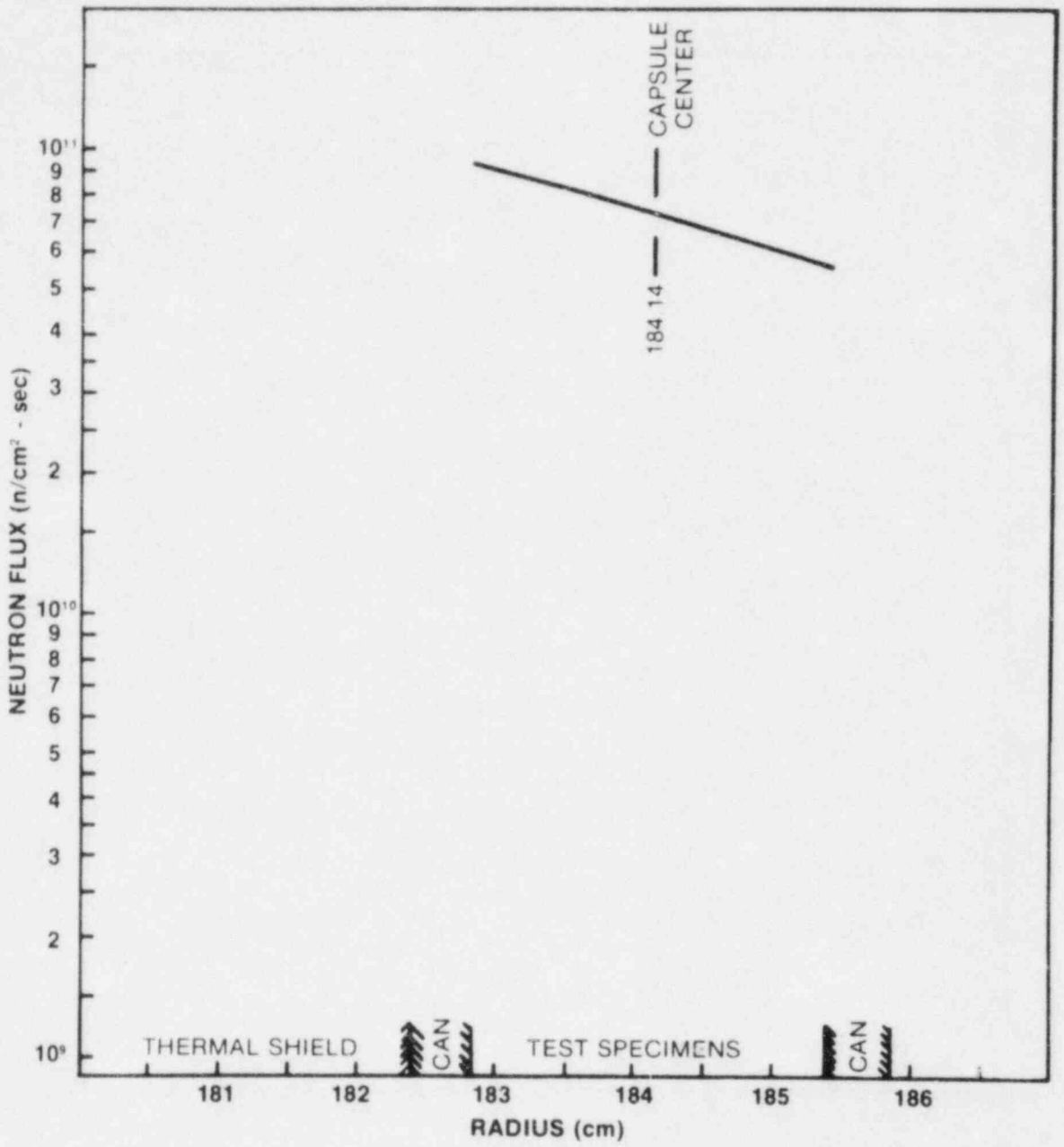

Figure 6-6. **Calculated radial distribution of Maximum Fast Neutron Flux ($E > 1.0$ Mev) within the surveillance capsules.**

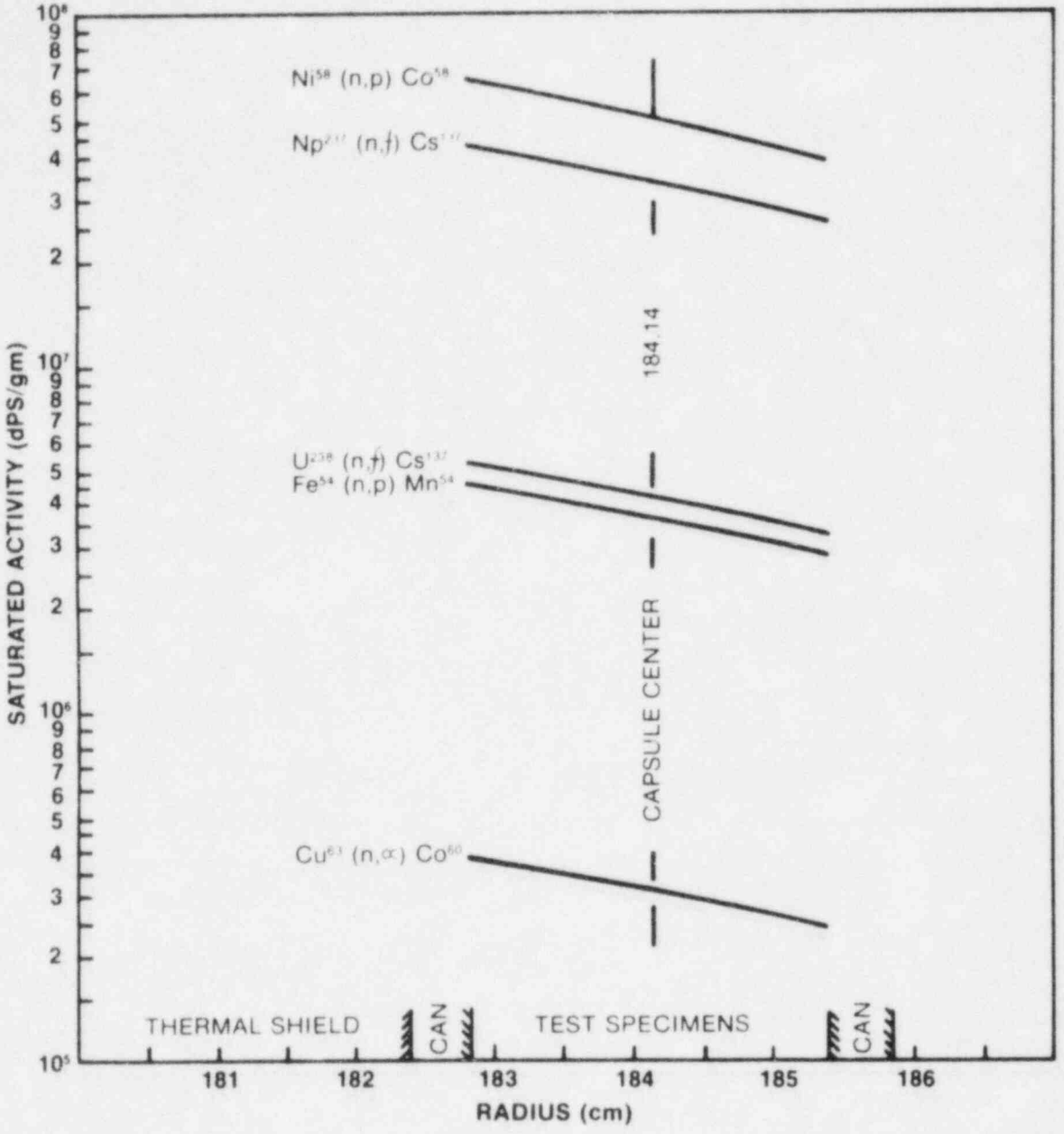

Figure 6-7. Calculated variation of Fast Neutron Flux Monitor saturated activity within the surveillance capsules.

6-5. DOSIMETRY RESULTS

The irradiation history of the Connecticut Yankee reactor is given in Table 6-6. Comparisons of measured and calculated saturated activity of the flux monitors contained in Capsules A, F, H, and D are listed in Tables 6-7, 6-8, 6-9 and 6-10, respectively. The data are presented as measured at the actual monitor locations as well as adjusted to the capsule center. The measured results for Capsule D were obtained by Westinghouse as an integral part of the current analysis, whereas, those for Capsules A, F, and H were derived from information presented in references 2, 3, and 4. All adjustments to the capsule center were based on the data given in Figure 6-7.

The fast neutron ($E > 1.0$ Mev) flux and fluence levels derived for Capsules A, F, H, and D are presented in Table 6-11. The thermal neutron flux obtained from the cobalt-aluminum monitors is summarized in Table 6-12. Due to the relatively low thermal neutron flux at the capsule locations, no burnup correction was made to any of the measured activities. The maximum error introduced by this assumption is estimated to be less than 1 percent for the Ni^{58} (n,p) Co^{58} reaction and even less significant for all of the other fast neutron reactions.

Using the iron data presented in Table 6-11 along with the lead factors given in Table 6-3, the fast neutron fluence ($E > 1.0$ Mev) for Capsules A, F, H, and D as well as for the reactor vessel inner diameter are summarized in Table 6-13 and Figure 6-8. An examination of Table 6-13 and Figure 6-8 shows that early in life the design basis transport analysis is quite conservative with respect to measurement and, in fact, overpredicts the capsule fluence by almost 80% for fuel cycle 1. However, later in life the agreement between calculation and measurement becomes very good with the analysis overpredicting the Capsule D data by only 7%. This improving trend is clearly illustrated in Figure 6-8. The discrepancies noted early in life are most likely due to lower peripheral power densities in the first and second cycle core designs. A further examination of Table 6-13 shows that the same conclusions would be reached if the basis of comparison were the average of all fast neutron dosimetry results rather than the iron results alone.

Projecting to end-of-life a summary of peak fast neutron exposure of the Connecticut Yankee reactor as derived from both calculation and Fe^{54} (n, p) Mn^{54} measurements from Capsule D may be made as follows.

	Fast Neutron Fluence (n/cm^2)		
	Surface	**1/4 T**	**3/4 T**
Capsule D	5.9×10^{19}	2.7×10^{19}	3.8×10^{18}
Calculation	6.3×10^{19}	2.9×10^{19}	4.1×10^{18}

These data are based on 27 full power years of operation at 1825 MWT.

From the results of tests performed to date, the following removal schedule is recommended for the remaining surveillance capsules.

Capsule Identification	Vessel Location	Lead Factor	Removal Date
B	46.5°	0.97	15EFPY
C	133.5°	0.97	20EFPY
E	223.5°	0.97	27EFPY
G	313.5°	0.97	Standby

TABLE 6-6

IRRADIATION HISTORY OF CONNECTICUT YANKEE REACTOR VESSEL SURVEILLANCE CAPSULES

Month — Year		P_j (MW)	P_{max} (MW)	P_j / P_{max}	Irradiation Time (days)	Decay Time (days)
10	1967	240.	1825	.132	31	5306
11	1967	621.	1825	.340	30	5276
12	1967	1399.	1825	.766	31	5245
1	1968	958.	1825	.525	31	5214
2	1968	1431.	1825	.784	29	5185
3	1968	80.	1825	.044	31	5154
4	1968	505.	1825	.277	30	5124
5	1968	1421.	1825	.778	31	5093
6	1968	1176.	1825	.644	30	5063
7	1968	1214.	1825	.665	31	5032
8	1968	944.	1825	.517	31	5001
9	1968	1180.	1825	.647	30	4971
10	1968	1460.	1825	.800	31	4940
11	1968	1247.	1825	.684	30	4910
12	1968	1248.	1825	.684	31	4879
1	1969	1430.	1825	.783	31	4848
2	1969	1411.	1825	.773	28	4820
3	1969	1580.	1825	.866	31	4789
4	1969	646.	1825	.354	30	4759
5	1969	765.	1825	.419	31	4728
6	1969	1120.	1825	.613	30	4698
7	1969	1228.	1825	.673	31	4667
8	1969	1272.	1825	.697	31	4636
9	1969	1431.	1825	.784	30	4606
10	1969	1573.	1825	.862	31	4575
11	1969	1422.	1825	.779	30	4545
12	1969	1733.	1825	.950	31	4514

TABLE 6-6 CONTINUED

IRRADIATION HISTORY OF CONNECTICUT YANKEE REACTOR VESSEL SURVEILLANCE CAPSULES

Month — Year		P_j (MW)	P_{max} (MW)	P_j/P_{max}	Irradiation Time (days)	Decay Time (days)
1	1970	1767.	1825	.968	31	4483
2	1970	1619.	1825	.887	28	4455
3	1970	1286.	1825	.704	31	4424
4	1970	695.	1825	.381	30	4394
Capsule A Removed						
5	1970	0.	1825	0.000	31	4363
6	1970	66.	1825	.036	30	4333
7	1970	1635.	1825	.896	31	4302
8	1970	1484.	1825	.813	31	4271
9	1970	1426.	1825	.781	30	4241
10	1970	1686.	1825	.924	31	4210
11	1970	1738.	1825	.952	30	4180
12	1970	1719.	1825	.942	31	4149
1	1971	1767.	1825	.968	31	4118
2	1971	1743.	1825	.955	28	4090
3	1971	1694.	1825	.928	31	4059
4	1971	817.	1825	.448	30	4029
Capsule F Removed						
5	1971	231.	1825	.127	31	3998
6	1971	1458.	1825	.799	30	3968
7	1971	1550.	1825	.849	31	3937
8	1971	1565.	1825	.858	31	3906
9	1971	1703.	1825	.933	30	3876
10	1971	1651.	1825	.905	31	3845

TABLE 6-6 CONTINUED

IRRADIATION HISTORY OF CONNECTICUT YANKEE REACTOR VESSEL SURVEILLANCE CAPSULES

Month — Year	P_j (MW)	P_{max} (MW)	P_j/P_{max}	Irradiation Time (days)	Decay Time (days)
11 1971	1785.	1825	.978	30	3815
12 1971	1706.	1825	.935	31	3784
1 1972	1729.	1825	.947	31	3753
2 1972	1710.	1825	.937	29	3724
3 1972	1766.	1825	.968	31	3693
4 1972	1759.	1825	.964	30	3663
5 1972	1704.	1825	.934	31	3632
6 1972	504.	1825	.276	30	3602
7 1972	775.	1825	.425	31	3571
8 1972	1720.	1825	.942	31	3540
9 1972	1517.	1825	.831	30	3510
10 1972	1768.	1825	.969	31	3479
11 1972	1578.	1825	.865	30	3449
12 1972	1768.	1825	.969	31	3418
1 1973	1761.	1825	.965	31	3387
2 1973	1602.	1825	.878	28	3359
3 1973	1774.	1825	.972	31	3328
4 1973	1751.	1825	.959	30	3298
5 1973	1753.	1825	.961	31	3267
6 1973	743.	1825	.407	30	3237
7 1973	353.	1825	.193	31	3206
8 1973	0.	1825	0.000	31	3175
9 1973	0.	1825	0.000	30	3145
10 1973	0.	1825	0.000	31	3114
11 1973	0.	1825	0.000	30	3084
12 1973	660.	1825	.362	31	3053

TABLE 6-6 CONTINUED

IRRADIATION HISTORY OF CONNECTICUT YANKEE REACTOR VESSEL SURVEILLANCE CAPSULES

Month — Year		P_j (MW)	P_{max} (MW)	P_j/P_{max}	Irradiation Time (days)	Decay Time (days)
1	1974	1679.	1825	.920	31	3022
2	1974	1692.	1825	.927	28	2994
3	1974	1257.	1825	.689	31	2963
4	1974	522.	1825	.286	30	2933
5	1974	1707.	1825	.935	31	2902
6	1974	1624.	1825	.890	30	2872
7	1974	1661.	1825	.910	31	2841
8	1974	1660.	1825	.909	31	2810
9	1974	1678.	1825	.920	30	2780
10	1974	1631.	1825	.893	31	2749
11	1974	1750.	1825	.959	30	2719
12	1974	1701.	1825	.932	31	2688
1	1975	1760.	1825	.964	31	2657
2	1975	1661.	1825	.910	28	2629
3	1975	1635.	1825	.896	31	2598
4	1975	1751.	1825	.959	30	2568
5	1975	852.	1825	.467	31	2537
6	1975	2.	1825	.001	30	2507
7	1975	1492.	1825	.818	31	2476
8	1975	1685.	1825	.924	31	2445
9	1975	1705.	1825	.934	30	2415
10	1975	1759.	1825	.964	31	2384
11	1975	1758.	1825	.964	30	2354
12	1975	1541.	1825	.844	31	2323
1	1976	1696.	1825	.929	31	2292
2	1976	1751.	1825	.959	29	2263

TABLE 6-6 CONTINUED

IRRADIATION HISTORY OF CONNECTICUT YANKEE REACTOR VESSEL SURVEILLANCE CAPSULES

Month — Year		P_j (MW)	P_{max} (MW)	P_j/P_{max}	Irradiation Time (days)	Decay Time (days)
3	1976	1749.	1825	.958	31	2232
4	1976	1582.	1825	.867	30	2202
5	1976	1006.	1825	.551	31	2171
6	1976	0.	1825	0.000	30	2141
7	1976	656.	1825	.360	31	2110
8	1976	1684.	1825	.923	31	2079
9	1976	1706.	1825	.935	30	2049
10	1976	1778.	1825	.974	31	2018
11	1976	1778.	1825	.974	30	1988
12	1976	1762.	1825	.965	31	1957
1	1977	1777.	1825	.974	31	1926
2	1977	1773.	1825	.971	28	1898
3	1977	1780.	1825	.975	31	1867
4	1977	1777.	1825	.974	30	1837
5	1977	1761.	1825	.965	31	1806
6	1977	1737.	1825	.952	30	1776
7	1977	1697.	1825	.930	31	1745
8	1977	1193.	1825	.654	31	1714
9	1977	1683.	1825	.922	30	1684
10	1977	760.	1825	.416	31	1653
		Capsule H Removed				
11	1977	0.	1825	0.000	30	1623
12	1977	1197.	1825	.656	31	1592
1	1978	1465.	1825	.803	31	1561
2	1978	1647.	1825	.902	28	1533

TABLE 6-6 CONTINUED

IRRADIATION HISTORY OF CONNECTICUT YANKEE REACTOR VESSEL SURVEILLANCE CAPSULES

Month — Year		P_j (MW)	P_{max} (MW)	P_j/P_{max}	Irradiation Time (days)	Decay Time (days)
3	1978	1587.	1825	.870	31	1502
4	1978	1750.	1825	.959	30	1472
5	1978	1733.	1825	.949	31	1441
6	1978	1465.	1825	.803	30	1411
7	1978	1703.	1825	.933	31	1380
8	1978	1688.	1825	.925	31	1349
9	1978	1710.	1825	.937	30	1319
10	1978	1777.	1825	.974	31	1288
11	1978	1757.	1825	.963	30	1258
12	1978	1775.	1825	.972	31	1227
1	1979	1503.	1825	.824	31	1196
2	1979	0.	1825	0.000	28	1168
3	1979	998.	1825	.547	31	1137
4	1979	1795.	1825	.984	30	1107
5	1979	1719.	1825	.942	31	1076
6	1979	1746.	1825	.957	30	1046
7	1979	1441.	1825	.790	31	1015
8	1979	1726.	1825	.946	31	984
9	1979	1641.	1825	.899	30	954
10	1979	1301.	1825	.713	31	923
11	1979	1795.	1825	.984	30	893
12	1979	1798.	1825	.985	31	862
1	1980	1796.	1825	.984	31	831
2	1980	1694.	1825	.928	29	802
3	1980	1721.	1825	.943	31	771
4	1980	1585.	1825	.869	30	741

TABLE 6-6 CONTINUED

IRRADIATION HISTORY OF CONNECTICUT YANKEE REACTOR VESSEL SURVEILLANCE CAPSULES

Month — Year		P_j (MW)	P_{max} (MW)	P_j/P_{max}	Irradiation Time (days)	Decay Time (days)
5	1980	115.	1825	.063	31	710
6	1980	0.	1825	0.000	30	680
7	1980	128.	1825	.070	31	649
8	1980	1484.	1825	.813	31	618
9	1980	1526.	1825	.836	30	588
10	1980	1786.	1825	.978	31	557
11	1980	1618.	1825	.887	30	527
12	1980	1761.	1825	.965	31	496
1	1981	1710.	1825	.937	31	465
2	1981	1714.	1825	.939	28	437
3	1981	1788.	1825	.980	31	406
4	1981	1768.	1825	.969	30	376
5	1981	1752.	1825	.960	31	345
6	1981	1731.	1825	.948	30	315
7	1981	1551.	1825	.850	31	284
8	1981	1567.	1825	.858	31	253
9	1981	1389.	1825	.761	30	223

Capsule D Removed

NOTE: Decay Time is referenced to the counting date of flux monitors removed from Capsule D.

TABLE 6-7

COMPARISON OF MEASURE AND CALCULATED FAST NEUTRON FLUX MONITOR SATURATED ACTIVITIES FOR CAPSULE A

Reaction and Axial Position	Radial Location (cm)	Saturated Activity (dPS/gm)		Adjusted Saturated Activity (dPS/gm)	
		Capsule A	Calculated	Capsule A	Calculated
Fe^{54} (n,p) Mn^{54}					
C-41	184.77	1.78×10^{6}	3.21×10^{6}	2.00×10^{6}	
C-44	184.77	1.90×10^{6}	3.21×10^{6}	2.13×10^{6}	
C-48	184.77	1.60×10^{6}	3.21×10^{6}	1.79×10^{6}	
Average				1.97×10^{6}	3.60×10^{6}
Ni^{58} (n,p) Co^{58}					
Bottom	184.77	2.96×10^{7}	4.41×10^{7}	3.36×10^{7}	5.01×10^{7}
Np^{237} (n,f) Cs^{137}					
Middle	184.14	2.03×10^{7}	3.34×10^{7}	2.03×10^{7}	3.34×10^{7}
U^{238} (n,f) Cs^{137}					
Middle	184.14	1.49×10^{6}	4.12×10^{6}	1.49×10^{6}	4.12×10^{6}

TABLE 6-8

COMPARISON OF MEASURED AND CALCULATED FAST NEUTRON FLUX MONITOR SATURATED ACTIVITIES FOR CAPSULE F

Reaction and Axial Position	Radial Location (cm)	Saturated Activity (dPS/gm)		Adjusted Saturated Activity (dPS/gm)	
		Capsule F	Calculated	Capsule F	Calculated
Fe^{54} (n,p) Mn^{54}					
C-24	184.77	2.46×10^{6}	3.21×10^{6}	2.76×10^{6}	
C-20	184.77	2.55×10^{6}	3.21×10^{6}	2.86×10^{6}	
C-17	184.77	2.44×10^{6}	3.21×10^{6}	2.74×10^{6}	
Average				2.79×10^{6}	3.60×10^{6}
Cu^{63} (n,α) Co^{60}					
Top	184.77	2.45×10^{5}	2.74×10^{5}	2.76×10^{5}	
Middle	184.77	2.70×10^{5}	2.74×10^{5}	3.04×10^{5}	
Bottom	184.77	2.54×10^{5}	2.74×10^{5}	2.86×10^{5}	
Average				2.89×10^{5}	3.09×10^{5}

TABLE 6-9

COMPARISON OF MEASURED AND CALCULATED FAST NEUTRON FLUX MONITOR SATURATED ACTIVITIES FOR CAPSULE H

Reaction and Axial Position	Radial Location (cm)	Saturated Activity (dPS/gm)		Adjusted Saturated Activity (dPS/gm)	
		Capsule H	Calculated	Capsule H	Calculated
Fe^{54} (n,p) Mn^{54}					
C-33	184.77	2.96×10^6	3.21×10^6	3.32×10^6	
C-40	184.77	2.74×10^6	3.21×10^6	3.07×10^6	
C-37	184.77	3.11×10^6	3.21×10^6	3.49×10^6	
R-33	183.77	3.20×10^6	3.86×10^6	2.98×10^6	
R-40	183.77	3.32×10^6	3.86×10^6	3.10×10^6	
R-37	183.77	3.67×10^6	3.86×10^6	3.42×10^6	
Average				3.23×10^6	3.60×10^6
Cu^{63} (n,α) Co^{60}					
Top	184.77	2.95×10^5	2.74×10^5	3.33×10^5	
Middle	184.77	3.12×10^5	2.74×10^5	3.52×10^5	
Average				3.43×10^5	3.09×10^5

TABLE 6-10

COMPARISON OF MEASURED AND CALCULATED FAST NEUTRON FLUX MONITOR SATURATED ACTIVITIES FOR CAPSULE D

Reaction and Axial Position	Radial Location (cm)	Saturated Activity (dPS/gm)		Adjusted Saturated Activity (dPS/gm)	
		Capsule D	Calculated	Capsule D	Calculated
Fe^{54} (n,p) Mn^{54}					
H-9	183.77	3.52×10^{6}	3.86×10^{6}	3.28×10^{6}	
H-12	183.77	3.82×10^{6}	3.86×10^{6}	3.56×10^{6}	
H-16	183.77	3.39×10^{6}	3.86×10^{6}	3.16×10^{6}	
Y-44	184.77	2.85×10^{6}	3.21×10^{6}	3.20×10^{6}	
Y-41	184.77	2.85×10^{6}	3.21×10^{6}	3.20×10^{6}	
Y-48	184.77	2.87×10^{6}	3.21×10^{6}	3.22×10^{6}	
Average				3.27×10^{6}	3.60×10^{6}
Ni^{58} (n,p) Co^{58}					
Bottom	184.77	4.65×10^{7}	4.41×10^{7}	5.28×10^{7}	5.01×10^{7}
Cu^{63} (n,α) Co^{60}					
Top	184.77	3.05×10^{5}	2.74×10^{5}	3.44×10^{5}	
Middle	184.77	3.05×10^{5}	2.74×10^{5}	3.44×10^{5}	
Bottom	184.77	2.95×10^{5}	2.74×10^{5}	3.33×10^{5}	
Average				3.40×10^{5}	3.09×10^{5}
Np^{237} (n,f) Cs^{137}					
Middle	184.14	2.58×10^{7}	3.34×10^{7}	2.58×10^{7}	3.34×10^{7}
U^{238} (n,f) Cs^{137}					
Middle	184.14	5.17×10^{6}	4.12×10^{6}	5.17×10^{6}	4.12×10^{6}

TABLE 6-11

RESULTS OF FAST NEUTRON DOSIMETRY FOR CAPSULES A, F, H, AND D

Capsule	Reaction	Adjusted Saturated Activity (dPS/gm)		ϕ (E > 1.0 Mev) (n/cm² - sec)		Φ (E > 1.0 Mev) (n/cm²)	
		Measured	Calculated	Measured	Calculated	Measured	Calculated
A	Fe^{54} (n,p) Mn^{54}	1.97×10^{6}	3.60×10^{6}	4.03×10^{10}	7.20×10^{10}	2.39×10^{18}	4.27×10^{18}
	Ni^{58} (n,p) Co^{58}	3.36×10^{7}	5.01×10^{7}	4.48×10^{10}	7.20×10^{10}	2.87×10^{18}	4.27×10^{18}
	Np^{237} (n,f) Cs^{137}	2.03×10^{7}	3.34×10^{7}	4.37×10^{10}	7.20×10^{10}	2.59×10^{18}	4.27×10^{18}
	U^{238} (n,f) Cs^{137}	1.49×10^{6}	4.12×10^{6}	2.66×10^{10}	7.20×10^{10}	1.58×10^{18}	4.27×10^{18}
F	Fe^{54} (n,p) Mn^{54}	2.79×10^{6}	3.60×10^{6}	5.70×10^{10}	7.20×10^{10}	4.71×10^{18}	5.95×10^{18}
	Cu^{63} (n,α) Co^{60}	2.89×10^{5}	3.09×10^{5}	7.07×10^{10}	7.20×10^{10}	5.85×10^{18}	5.95×10^{18}
H	Fe^{54} (n,p) Mn^{54}	3.23×10^{6}	3.60×10^{6}	6.60×10^{10}	7.20×10^{10}	1.58×10^{19}	1.72×10^{19}
	Cu^{63} (n,α) Co^{60}	3.43×10^{5}	3.09×10^{5}	8.39×10^{10}	7.20×10^{10}	2.01×10^{19}	1.72×10^{19}
D	Fe^{54} (n,p) Mn^{54}	3.27×10^{6}	3.60×10^{6}	6.68×10^{10}	7.20×10^{10}	2.22×10^{19}	2.39×10^{19}
	Ni^{58} (n,p) Co^{58}	5.28×10^{7}	5.01×10^{7}	7.61×10^{10}	7.20×10^{10}	2.53×10^{19}	2.39×10^{19}
	Cu^{63} (n,α) Co^{60}	3.40×10^{5}	3.09×10^{5}	8.32×10^{10}	7.20×10^{10}	2.76×10^{19}	2.39×10^{19}
	Np^{237} (n,f) Cs^{137}	2.58×10^{7}	3.34×10^{7}	5.56×10^{10}	7.20×10^{10}	1.85×10^{19}	2.39×10^{19}
	U^{238} (n,f) Cs^{137}	5.17×10^{6}	4.12×10^{6}	9.24×10^{10}	7.20×10^{10}	3.07×10^{19}	2.39×10^{19}

TABLE 6-12

RESULTS OF THERMAL NEUTRON DOSIMETRY FOR CAPSULES A, F, H, AND D

Capsule	Axial Location	Saturated Activity (dPS/gm)		ϕTH (n/cm^2 - sec)
		Bare	Cd - Covered	
A	Average	—	—	2.12×10^{10}
F	Average	—	—	2.86×10^{10}
H	Average	6.17×10^{7}	2.15×10^{7}	7.10×10^{10}
D	Average	5.96×10^{7}	2.09×10^{7}	6.83×10^{10}

NOTE: Thermal Flux Data for Capsules A and F were not re-evaluated.

TABLE 6-13

SUMMARY OF FAST NEUTRON DOSIMETRY RESULTS FOR SURVEILLANCE CAPSULES A, F, H, D BASED ON THE Fe^{54} (n,p) Mn^{54} REACTION

Capsule	Irradiation Time (EFPS)	ϕ(E > 1.0 Mev) (n/cm² - sec)	Φ (E> 1.0 Mev) (n/cm²)	Lead Factor	Vessel Fluence (n/cm²)	Calculated Vessel Fluence (n/cm²)
A	5.93×10^{7}	4.03×10^{10}	2.39×10^{18}	0.97	2.46×10^{18}	4.40×10^{18}
F	8.27×10^{7}	5.70×10^{10}	4.71×10^{18}	0.97	4.86×10^{18}	6.14×10^{18}
H	2.39×10^{8}	6.60×10^{10}	1.58×10^{19}	0.97	1.63×10^{19}	1.77×10^{19}
D	3.32×10^{8}	6.68×10^{10}	2.22×10^{19}	0.97	2.29×10^{19}	2.46×10^{19}

BASED ON THE AVERAGE OF ALL FAST NEUTRON REACTIONS

Capsule	Irradiation Time (EFPS)	ϕ (E > 1.0 Mev) (n/cm² - sec)	Φ (E > 1.0 Mev) (n/cm²)	Lead Factor	Vessel Fluence (n/cm²)	Calculated Vessel Fluence (n/cm²)
A	5.93×10^{7}	3.98×10^{10}	2.36×10^{18}	0.97	2.43×10^{18}	4.40×10^{18}
F	8.27×10^{7}	6.39×10^{10}	5.28×10^{18}	0.97	5.44×10^{18}	6.14×10^{18}
H	2.39×10^{8}	7.49×10^{10}	1.79×10^{19}	0.97	1.85×10^{19}	1.77×10^{19}
D	3.32×10^{8}	7.48×10^{10}	2.48×10^{19}	0.97	2.56×10^{19}	2.46×10^{19}

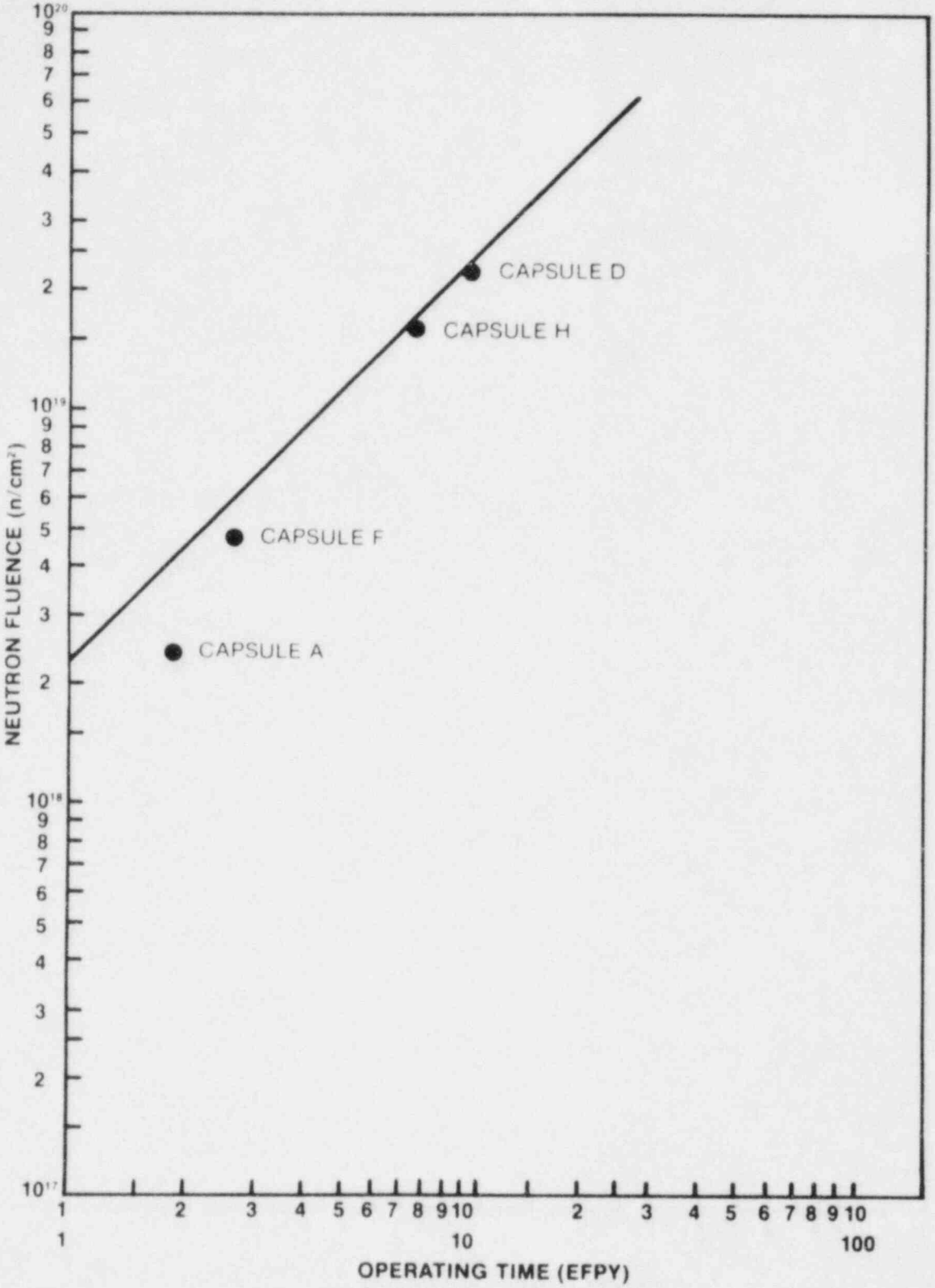

Figure 6-8. **Comparison of measured and calculated Fast Neutron Fluence (E > 1.0 Mev) within the surveillance capsules.**

REFERENCES

1. Yanichko, S.E., "Connecticut Yankee Reactor Vessel Radiation Surveillance Program," WCAP-7036, April, 1967.

2. Ireland, D.R., and Scotti, V.G., "Examination and Evaluation of Capsule A for the Connecticut Yankee Reactor Pressure-Vessel Surveillance Program," Battelle Memorial Institute Report, October 30, 1970.

3. Perrin, J.S. etal, "Examination and Evaluation of Capsule F for the Connecticut Yankee Reactor Pressure-Vessel Surveillance Program," Battelle Columbus Laboratories Report, March 30, 1972.

4. Fields, P.J., and Anderson, S.L. "Analysis of Capsule H from the Connecticut Yankee Reactor Vessel Radiation Surveillance Program," WCAP-9339, September, 1978.

5. Soltesz, R.G., R.K. Disney, J. Jedruch, and S.L. Zeigler, "Nuclear Rocket Shielding Methods, Modification, Updating and Input Data Preparation — Volume 5 — Two-Dimensional, Discrete Ordinates Transport Technique," WANL-PR-(LL)-034, Vol. 5, August 1970.

6. Collier, G., G. Gibson, L.L. Moran, R.K. Disney, and R.S. Kaiser, "Second Version of the GAMB1T Code, WANL-TME-1969, November 1969.

7. Soltesz, R.G., R.K. Disney, S.L. Zeigler, "Nuclear Rocket Shielding Methods, Modification, Updating and Input Data Preparation — Volume 3, Cross-Section Generation and Data Processing Techniques," WANL-PR-(LL)-034, August 1970.

8. Soltesz, R.G. and R.K. Disney, "Nuclear Rocket Shielding Methods, Modification, Updating and Input Data Preparation — Volume 4 — One-Dimensional Discrete Ordinates Transport Technique," WANL-PR-(LL)-034, August 1970.

9. ASTM Designation E261-70, Standard Method for Measuring Neutron Flux by Radioactivation Techniques," in ASTM Standards (1975), Part 45, Nuclear Standards, pp. 745-755, American Society for Testing and Materials, Philadelphia, Pa., 1975.

10. ASTM Designation E262-70, "Standard Method for Measuring Thermal Neutron Flux by Radioactivation Techniques," in ASTM Standards (1975), Part 45, Nuclear Standards, pp. 756-763, American Society for Testing and Materials, Philadelphia, Pa., 1975.

11. ASTM Designation E263-70, "Standard Method for Measuring Fast-Neutron Flux by Radioactivation of Iron," in ASTM Standards (1975), Part 45, Nuclear Standards, pp. 764-769, American Society for Testing and Materials, Philadelphia, Pa., 1975.

12. ASTM Designation E481-73T, "Tentative Method of Measuring Neutron-Flux Density by Radioactivation of Cobalt and Silver," in ASTM Standards (1975), Part 45, Nuclear Standards, pp. 887-894, American Society for Testing and Materials, Philadelphia, Pa., 1975.

13. ASTM Designation E264-70, "Standard Method for Measuring Fast-Neutron Flux by Radioactivation of Nickel," in ASTM Standards (1975), Part 45, Nuclear Standards, pp. 770-774, American Society for Testing and Materials, Philadelphia, Pa., 1975.